1-1-2005

Isolation and melting properties of branched fatty esters from lanolin

Linxing Yao
Iowa State University

Isolation and melting properties of branched fatty esters from lanolin

by

Linxing Yao

A thesis submitted to the graduate faculty

in partial fulfillment of the requirements for the degree of

MASTER OF SCIENCE

Major: Food Science and Technology

Program of Study Committee:
Lawrence A. Johnson, Major Professor
Earl G. Hammond
George A. Kraus
Basil J. Nikolau

Iowa State University

Ames, Iowa

2005

Graduate College
Iowa State University

This is to certify that the master's thesis of

Linxing Yao

has met the thesis requirements of Iowa State University

Signatures have been redacted for privacy

Table of Content

Introduction

The use of biodiesel to replace petroleum-based fuels has been given more and more attention in recent years because of the security of the energy supply and the deterioration of the global environment conditions and the concerns about renewability. But the disadvantages of biodiesel, such as its crystallization at low temperatures, its susceptibility to oxidation and its high cost, have retarded its development and application. There is growing interest in using the derivatives of *iso*- and *anteiso*-methyl-branched fatty acids in lubricants and industrial fluids to replace petroleum-based products, and others at Iowa State University are exploring the expression of these branched fatty acids in oilseed crops. The branched acids have the advantages of being biodegradable, and stable to oxidation. Branched fatty acids and their derivatives supposedly have lower melting points than their straight-chain counterparts. Thus, they perform better at low temperatures and may be an ideal raw material for biodiesel, but physical property data for branched acids and their esters is limited. At present, the only available data is the melting point of branched acids and their amides isolated from wool wax (1).

Wool wax is an important natural source of branched-chain fatty acids (2). Wool wax is a by-product recovered of the scouring of sheep's wool and is a complex mixture of high molecular weight, water-insoluble wax esters. Refined wool wax was patented as Lanolin by Liebreich and Braun in 1882 (3). The major components of lanolin are wax esters (75-90%) of long chain acids and long chain alcohols. The acids in the wax typically consisted of branched-chain and normal chain acids and α and ω-hydroxy acids esterified with lanosterol, cholesterol, branched alkanols and α , β -alkanediols. The minor components in lanolin include free fatty acids, free alcohols and hydrocarbons (1, 3). The branched-chain acids in

lanolin are mainly two types, *iso-* (isopropyl branch) and *anteiso-* (butyl branch), which have one methyl group on ω-2 and ω-3 position respectively (Fig. 1).

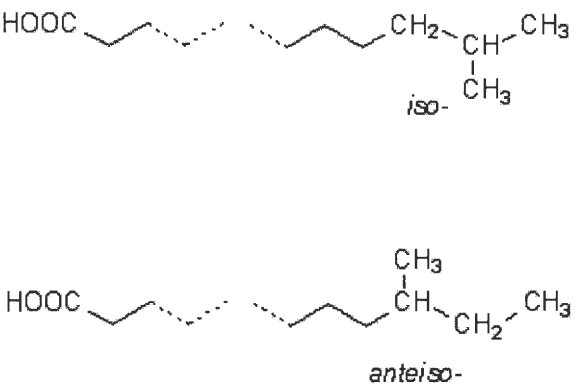

Fig. 1. Structure of *iso-* and *anteiso-* branched fatty acid

In this study, a complex mixture of branched methyl esters was obtained from lanolin through saponification, extraction of unsaponifiables with heptane and methylation. Hydroxy compounds were removed by chromatography on alumina. Vacuum spinning-band distillation separated the mixture roughly by chain length. Counter-current urea complex formation and crystallization separated individual methyl esters. Transesterification was used to convert methyl esters to isopropyl esters. The melting point and heat of fusion of each ester were determined by differential scanning calorimeter (DSC). ^{13}C nuclear magnetic resonance (NMR) and ^{1}H NMR were used to verify the structure of branched-chain esters.

Literature review

The use of fatty acid derivatives for biodiesel and industrial fluids

In recent years, environmental concern about petroleum-based fuels has encouraged the development of biodiesel, a promising and renewable alternative fuel for use in compression ignition (diesel) engines. Biodiesel is generally the methyl esters derived from vegetable oils or animal fats (4). The fatty acids in vegetable oils or animal fats are transesterified with a monohydric alcohol (generally methanol), catalyzed by sodium or potassium hydroxide, producing fatty acid alkyl esters and glycerol. The first example of vegetable oils in diesel engines dates back to the late eighteen century, when Rudolf Diesel (1858~1913) powered an engine with peanut oil (5). The petroleum fuels supply crisis of the 1970s, ignited a huge interest for alternative fuels from domestic resources. In 1988, rapeseed oil methyl ester was produced commercially as the first type of biodiesel fuel that was a biorevewable single-feed-stock product. The feedstocks for biodiesel are usually from the predominated oil products in a region. Rapeseed oil is used in Europe, sunflower oil in southern France and Italy, soybean oil in United States, palm oil in Malaysia and tropical areas, etc (4).

Biodiesel behaves similarly to petroleum diesel and in some ways is superior. Biodiesel offers similar power to diesel fuel. It has a higher cetane number than U.S.diesel fuel (The cetane number is "an indication of a fuels readiness to autoignite after it has been injected into a diesel engine".) (6). Also, biodiesel provides excellent lubricity and a higher flash point, which are desired properties for fuels. Biodiesel is produced from renewable sources that can decrease the reliance on imported petroleum, in other words, increase the

supply security of fuel. In addition, and more important, biodiesel greatly benefits the environment because it contains no sulfur or aromatics and it has closed carbon cycle. Thus, it substantially reduces the emission of unburned hydrocarbons, carbon monoxide and particulate matter and contributes less to air pollution and global warming. Biodiesel degrades in the environment four times faster than ordinary diesel, which reduces health risks and environmental stress (6).

In spite of these advantages, there are some considerations limiting the commercialization of biodiesel in the United States. Problems include biodiesel's high cost, oxidative stability and low temperature performance (below 0°C). Soy diesel, based on blends of methyl soyate, which is the methyl ester of soybean oil, crystallizes at ~0°C. The 14-16% saturated fatty acids in typical soybean oil contribute to the high crystallization temperature of soy diesel and cause fuel lines and filters to become plugged at cold temperatures.

A great amount of research has been done to improve the cold temperature performance of biodiesel. Relying on double bonds to decrease the melting point makes the hydrocarbon chains subject to oxidation. Oxidation is particularly a problem in methylene interrupted polyunsaturated fatty acids, and *cis, cis*-9,12-octadecadienoic acid (linoleic acid) oxidizes about 10 times faster than *cis*-9-octadecenoic acid (oleic acid) (7, 8). The crystallization properties of biodiesel fuels can be improved by using high-oleic oils, since monounsaturated esters present optimum oxidative stability and lower melting points compared to saturated fatty esters.

An alternative to increasing unsaturation is inducing branches by replacing methyl or ethyl esters with the branched-chain alcohols, such as isopropanol (9). The branches change

the molecular packing and intermolecular interaction so that the crystallization temperature reduced. Isopropyl and 2-butyl esters of normal soybean oil crystallized 7-14°C lower than corresponding normal chain methyl ester. Winterization is another alternative that can reduce the crystallization temperature by removing the saturated methyl esters through a cooling and filtration process. Winterizing normal soybean oil with diluted hexane depressed crystallization temperature by 9°C with 77% yield. A 10°C reduction on crystallization temperature was obtained by winterizing low-palmitate soybean oil with 86% yield (10).

Factors affecting the melting points of lipids

The melting point of normal saturated fatty acids increase with chain length, and capric acid (C10:0) with a melting point of 31.6°C marks the divide between those that are liquid and solid at room temperature. At the more common chain lengths of 16 and 18, melting points reach values of 62.9°C and 70.1°C, respectively. The heat of fusion measures the amount of heat required to melt solid at its melting point with no change in temperature. The heat of fusion increases with molecular weight. The normal saturated fatty acids with chain length of 10, 16 and 18 need 28.0, 54.4 and 63.2 kJ/mol respectively, at their melting point (11).

Almost all fatty acids are polymorphic, which means that they possess two or more crystal forms under certain thermodynamical conditions. Polymorphism is defined as "the ability to reveal different unit cell structures in crystals, originating from a variety of molecular conformations and molecular packings" (12). Both melting point and heat of fusion of a particular fatty acid vary with polymorphism. Typically, rapid cooling process gives an unstable polymorphic crystal form with lower melting point and heat of fusion; whereas, slow cooling encourages the formation of a stable crystal which has a higher

melting point and heat of fusion. The heat of fusion of α, β', and β (of which α is the least unstable form, β is the most stable form, and β' is the intermediate form.) polymorphic form of glyceryl tristearale were 109.3 142.8, and 188.4 kJ/mol (13).

The introduction of double bonds into a fatty acid prevents the easy alignment of the fatty acid chain in crystals and lowers the melting point considerably with melting points for *cis*- and *trans*-9-octadecenoic acid (oleic acid) reported at 16.25 and 43.68˚C, respectively (14). Based on the knowledge of how unsaturation affects the melting point, one might assume that branched chains also would greatly lower the melting points, since branches also prevent close chain packing. According to Weitkamp, the melting point of even-chain methyl branched *iso*-fatty acids were quite close to those with a normal chain; whereas odd-chain *anteiso*-branched fatty acids had significantly lower melting points (1). The heat of fusion of branched acid from natural sources was not previously available.

The occurrence and distribution of branched acids

Branched chain fatty acids occur widely in nature. The naturally occurring branched chain fatty acids were first discovered by Anderson and Chargaff during the period 1929-1930 (15). The acid, which they isolated from the lipids of human tubercle bacillus, was 10-methylstearic acid. Later, other branched chain acids were found in this and other bacteria (16, 17), in wool wax (1), in mutton and butter fat (18, 19, 20), in shark liver oil (18, 21, 22), in ox fat (18, 23), and in human skin (24). Branched acids are rarely present in plant lipids. A single methyl group is the most common type of branching occurring in nature. *Iso*- acids (mainly with an even number of carbon atoms) and the *anteiso*- acids (mainly with an odd number of carbon atoms) occur widely in wool wax, other animal fats and some bacteria. These kinds of acids were found to be major components in wool wax (1) and present

significant in amounts in human skin lipid (2). A methyl group occurring at other positions is possible, such as 10-methylstearic acid (tuberculostearic acid) in bacteria and others in marine oil. Polymethyl branched acids with more than one methyl groups were found in the subcutaneous adipose tissue of ruminants, particularly on a barley-rich diet, uropygial wax produced by preen gland of birds, and bacterial lipids (2). These branched acids are thought to be produced by a modification of the normal *de novo* methyl malonate pathway. In addition, a group of branched acids, based on the diterpene phytol, is present at low levels in fish oils, milk and blood lipids. They are different from the groups discussed above in that they are not produced through the normal *de novo* fatty acid pathway (2, 25).

The isolation and identification of branched chain fatty acids

Although branched acids occur widely in nature, they usually are present at insignificant levels or in a highly complex mixture of lipid. The isolation of pure individual acids from natural sources has been difficult, and this has become an obstacle of further study the properties and applications of branched acids. In early work, normal and branched chain acids were separated by making use of the solubility of their lead salts (26). Distillation could not yield pure individual acid from a mixture of normal, monosaturated, and branched-chain acids (27). Urea complexation and column chromatography on aluminum oxide were used to separate normal and branched chain components (28).

Research conducted to isolate and identify branched acids from wool wax (degras or lanolin) began as early as 1870's. But the effective qualification and quantification study was done during the 1940s-1960s with the help of modern analytical methods. Weitkamp used low-pressure fractional distillation to separate the methyl esters of lanolin acids into a series of fractions. Then the methyl esters were converting to free acids and α-hydroxy acids were

removed by crystallization from petroleum ether and oxidation by potassium permanganate. Reesterified normal and branched chain acids were separated in an "extended distillation" by co-distillation with hydrocarbons. Identification of the acids was based on their crystal habits, molecular weights and melting points. Downing *et al*. (29) identified the branched chain acids in wool wax by reducing the methyl esters of wool wax acids to the corresponding hydrocarbons and then using gas chromatography (GC) to determine the composition of hydrocarbon mixtures. Ivserson *et al*. (30) separated lanolin acids into 15 successive fractions with urea-methanol by adjusting the amount of urea and volume of methanol. The separation was monitored by GC analysis. Pelick and Shigley (31) determined the composition of the fatty acids of degras by using a combination of thin-layer chromatography (TLC) and GC.

Weitkamp's work and its limitation

Weitkamp's work provided invaluable information on the isolation of branched chain acids and their physical properties; however, the research conditions at his time, such as the lack of gas chromatography, limited his work. The purity of the individual branched acids he isolated was based on their acid values. Weitkamp did not provide data on the melting points of methyl esters, which are of greater interest to the biodiesel industry. In addition, Weikamp's distillation column was considered to have a high hold-up volume, which means that some minor fractions would not have been separated.

Saponification and methylation of lanolin

Since lanolin consists of sterol and wax esters, it is difficult to saponify and remove unsaponifiables by traditional methods. Barnes *et al*. (32) found optimum methods for producing lanolin fatty acids from a laboratory scale to an industrial scale. He suggested that the operation of saponification and subsequent separation be done under very carefully

controlled conditions to accomplish completed saponification. Sodium hydroxide in ethanol was the optimum reagent. Both the reaction time and separation of unsaponifiables depended on the ratio of alkali/ethanol and excess alkali. During separation of unsaponifiables, the ratio of ethanol/water and the temperature of mixture must be controlled; otherwise undesired phase distributions and emulsions form that severely affected the yield of fatty acids. Barnes procedure was substantially used by the subsequent investigators (29, 31).

Analyses of the fatty acid composition of lanolin

The fatty acids in lanolin primarily consist of four homologous series as Weitkamp first showed (1): normal chain acids, α-hydroxy acids, *iso*-branched acids, and *anteiso*-branched acids. Among the non-hydroxylated acid groups, the *iso*- acids were found to be made up of acids ranging from C10 through C32 with C16, C18, C20 and C26 *iso*- acids as the major components, and the *anteiso*- acids range from C9 through C33 with C15, C19, C21, C25 and C27 as the major components (1, 29, 31).

Normal C14 and C16 α-hydroxy acids were isolated in Weitkamp's work (1). Horn *et al*. (33) isolated even chain normal α-hydroxy acids from C12 to C18, and the *iso*-C18 α-hydroxy acid. Additional normal α-hydroxy acids from C14 to C24, *iso*-α-hydroxy acids from C14 to C24, and *anteiso*-α-hydroxy acids from C15 to C25 were found later (29). Normal C16 and *iso*- C18 α-hydroxy acids were the dominant components.

In addition to the four acid series above, the presence of ω-hydroxy acids in lanolin were reported (34). This series of acids included normal chain acids as well as branched-chain (*iso*- and *anteiso*-) acids with normal C30, C32 and *anteiso*-C31 as the major constituents (29, 34).

The acids in wool wax was reported to consist of 10% normal chain acids, 21% *iso*-branched acids, 28% *anteiso*-branched acids and 30% α-hydroxyl acids by weight (29). Iverson *et al*. (30) reported the weight percentage of normal, branched, and hydroxy acids was 22%, 25% (*iso*-), 21% (*anteiso*-), and 33%. In Weitkamp's work, the normal, *iso*- and *anteiso*- acids were 10%, 30%, and 37%, respectively (1). About 30% of hydroxyl acids were separated from wool wax acids by Horn *et al* (35). Since lanolin is a natural product, the percentage of components varies. Limitation on gas chromatography, the methods used for recovery and unknown components also affect the analysis. The terminology of major branched-chain non-hydroxy acids in wool wax was given in Table 1.

The *anteiso*-branched acids identified by Weitkamp were found to be dextrorotatory (42). α-Hydroxy acids of C14 and C16 were determined as optically active (1, 36).

Table 1. The terminology and abbreviation of major *iso*- and *anteiso*-acids and their derivatives in wool wax

Carbon #	Acid	Fomula of FA	Methyl ester	Formula of ME	Abrr.
C10	8-methylnonanoic acid	$C_{10}H_{20}O_2$	8-methylnonanoic acid methyl ester	$C_{11}H_{22}O_2$	*iso*-C10, C10i
C11	8-methyldecanoic acid	$C_{11}H_{22}O_2$	8-methyldecanoic acid methyl ester	$C_{12}H_{24}O_2$	*ante*-C11, *anteiso*-C11, C11a
C12	10-methylundecanoic acid	$C_{12}H_{24}O_2$	10-methylundecanoic acid methyl ester	$C_{13}H_{26}O_2$	*iso*-C12, C12i
C13	10-methyldodecanoic acid	$C_{13}H_{26}O_2$	10-methyldodecanoic acid methyl ester	$C_{14}H_{28}O_2$	*ante*-C13, *anteiso*-C13, C13a
C14	12-methyltridecanoic acid	$C_{14}H_{28}O_2$	12-methyltridecanoic acid methyl ester	$C_{15}H_{30}O_2$	*iso*-C14, C14i
C15	13-methyltetradecanoic acid	$C_{15}H_{30}O_2$	13-methyltetradecanoic acid methyl ester	$C_{16}H_{32}O_2$	*iso*-C15, C15i
C15	12-methyltetradecanoic acid	$C_{15}H_{30}O_2$	12-methyltetradecanoic acid methyl ester	$C_{16}H_{32}O_2$	*ante*-C15, *anteiso*-C15, C15a
C16	14-methylpentadecanoic acid	$C_{16}H_{32}O_2$	14-methylpentadecanoic acid methyl ester	$C_{17}H_{34}O_2$	*iso*-C16, C16i
C17	15-methylhexadecanoic acid	$C_{17}H_{34}O_2$	15-methylhexadecanoic acid methyl ester	$C_{18}H_{36}O_2$	*Iso*-C17, C17i
C17	14-methylhexadecanoic acid	$C_{17}H_{34}O_2$	14-methylhexadecanoic acid methyl ester	$C_{18}H_{36}O_2$	*ante*-C17, *anteiso*-C17, C17a
C18	16-methylheptadecanoic acid	$C_{18}H_{36}O_2$	16-methylheptadecanoic acid methyl ester	$C_{19}H_{38}O_2$	*iso*-C18, C18i
C19	17-methyloctadecanoic acid	$C_{19}H_{38}O_2$	17-methyloctadecanoic acid methyl ester	$C_{20}H_{40}O_2$	*iso*-C19, C19i
C19	16-methyloctadecanoic acid	$C_{19}H_{38}O_2$	16-methyloctadecanoic acid methyl ester	$C_{20}H_{40}O_2$	*ante*-C19, *anteiso*C19, C19a
C20	18-methylnonadecanoic acid	$C_{20}H_{40}O_2$	18-methylnonadecanoic acid methyl ester	$C_{21}H_{42}O_2$	*iso*-C20, C20i
C21	18-methyleicosanoic acid	$C_{21}H_{42}O_2$	18-methyleicosanoic acid methyl ester	$C_{22}H_{44}O_2$	*ante*-C21, *anteiso*-C21, C21a
C22	20-methylheneicosanoic acid	$C_{22}H_{44}O_2$	20-methylheneicosanoic acid methyl ester	$C_{23}H_{46}O_2$	*iso*-C22, C22i
C23	20-methyldocosanoic acid	$C_{23}H_{46}O_2$	20-methyldocosanoic acid methyl ester	$C_{24}H_{48}O_2$	*ante*-C23, *anteiso*-C23, C23a
C24	22-methyltricosanoic acid	$C_{24}H_{48}O_2$	22-methyltricosanoic acid methyl ester	$C_{25}H_{50}O_2$	*iso*-C24, C24i
C25	22-methyltetracosanoic acid	$C_{25}H_{50}O_2$	22-methyltetracosanoic acid methyl ester	$C_{26}H_{52}O_2$	*ante*-C25, *anteiso*-C25, C25a
C26	24-methylpentacosanoic acid	$C_{26}H_{52}O_2$	24-methylpentacosanoic acid methyl ester	$C_{27}H_{54}O_2$	*iso*-C26, C26i
C27	24-methylhexacosanoic acid	$C_{27}H_{54}O_2$	24-methylhexacosanoic acid methyl ester	$C_{28}H_{56}O_2$	*ante*-C27, *anteiso*-C27, C27a
C28	26-methylheptacosanoic acid	$C_{28}H_{56}O_2$	26-methylheptacosanoic acid methyl ester	$C_{29}H_{58}O_2$	*iso*-C28, C28i
C29	26-methyloctacosanoic acid	$C_{29}H_{58}O_2$	26-methyloctacosanoic acid methyl ester	$C_{30}H_{60}O_2$	*ante*-C29, *anteiso*-C29, C29a
C30	28-methylnonacosanoic acid	$C_{30}H_{60}O_2$	28-methylnonacosanoic acid methyl ester	$C_{31}H_{62}O_2$	*iso*-C30, C30i
C31	28-methyltriacontanoic acid	$C_{31}H_{62}O_2$	28-methyltriacontanoic acid methyl ester	$C_{32}H_{64}O_2$	*ante*-C31, *anteiso*-C31, C31a

Separation techniques for fatty acids

Distillation

In earlier times, distillation was often used in industry to remove odors and contaminates having low boiling points. As more sophisticated fractionation equipment developed, distillation became an important separation and purification technique for fatty acids. Since fractional distillation was based upon differences in the boiling points of acids, it is possible to separate mixed acids by their chain length. Distillation is not good at separating components by their degree of saturation (37). Fractional distillation under reduced pressure is widely used today because it prevents polymerization, and lowers the temperature needed, although 200˚C is still generally required even under reduced pressure. Popular distillation columns include packed columns and spinning band columns. Packed columns, such as the one used by Weitkamp, have intersecting channel made up of parallel layers which distribute the refluxing liquid flowing down evenly over the column. Such columns have a significant hold-up, liquid undergoing fractionation in the column. This limits the recovery of small components in a pure state. Spinning band distillation column utilized a helical shaped Teflon band through the length of the column. The spinning band increases the number of theoretical plates and therefore obtains better equilibration between the components with different boiling points (Fig. 2). Thus, it is superior to packed column from the point of view of hold-up.

Urea complexes and counter-current urea complexing

Since urea was found to form complex with 1-octanol in 1940 (38, 39), urea complex formation has been developed to be an inexpensive, environmentally favorable alternative for

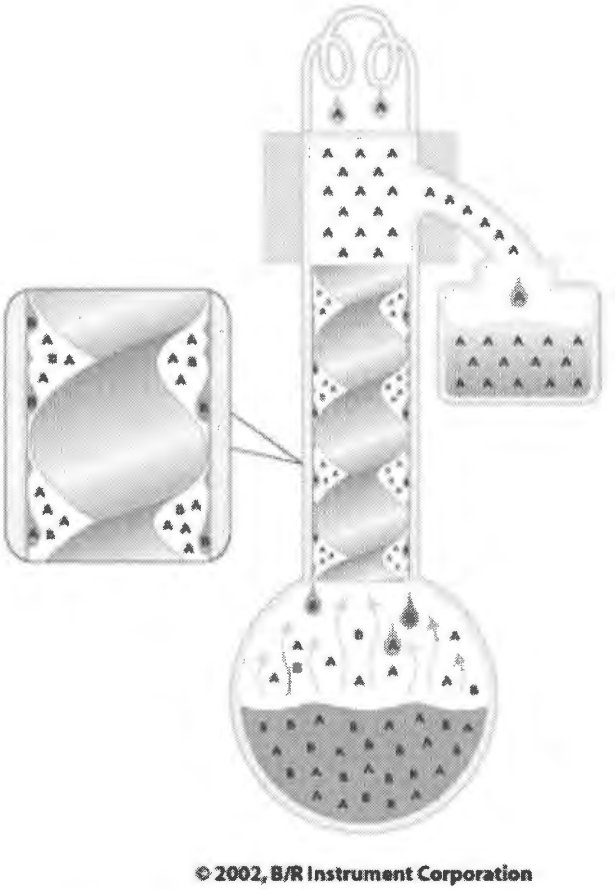

Fig. 2. Structure of spinning band column

fractionating free fatty acids (FFA) and their derivatives from various seed oil, fish oil, and other oils. Urea complexes also protected fatty acids from oxidation (40, 41).

Under certain conditions, helical-shaped urea complexes form between urea molecules and certain aliphatic compounds (37, 40). Pure urea normally has a tetragonal crystalline structure. In such a complex, six urea molecules bond together via hydrogen bonding and form a unit cell (1.11nm long and 0.82nm in outside diameter) containing a channel in which a linear molecule, serving as a template may be held if it fulfils certain dimensional qualifications. Strong van der Waals attractions and hydrogen bonding hold the

urea molecules and the templates in the hexagonal crystalline structure. The resultant urea clathrate is a needle-like crystals, consisting of a series of parallel channels. Molecules that are not too short or too long and whose width fits the channel can readily form complexes with urea. Typically, molecules having diameters of 0.4-0.6 nm, such as many straight-chain acids and their esters, are good templates. The ease of forming complex depends on the chain length, branched group, cyclic group, *cis* or *trans* double bonds, and stereochemistry of the compounds (40). When raised above a critical temperature, urea complexes discompose. In practice, saturated acids form complexes easier than unsaturated acids. Oleic acid enters the channel more readily than polyunsaturated acids. And straight chain acids fit dimension requirements much better than cyclic and branched acids. FFA of chain lengths less than 6-8 or containing constituents such as double bonds, as well as epoxy or hydroxy functional groups, are regarded to be less likely to form complexes. However, whether those "poor guest" can form urea complex is uncertain. The current acceptable explanation suggests that the present of "good guest" in a mixture may help the "poor guests" to be incorporated into the complex, or the "poor guest" may form only a loose type of complex that does not require the creation of a crystalline urea lattice along the entire length of the molecule (40). The formation of urea complex usually involves an appropriate solvent and elevated temperature to dissolve both urea and "guest". The preferred solvent is polar and thus unlikely to become a guest. Methanol is most frequently used. The complex forms during cooling to room temperature or a lower temperature. The desired cooling rate and final temperature is decided by the properties of guests and experimental purposes.

The major application of urea complex to fractionate FFA involves the isolation of polyunsaturated fatty acid, such as eicosapentaenoic acids (EPA) and docosahexaenoic acids

(DPA), cyclic acids, such as sterculic acids, α- and γ-linolenic acids from all kinds of vegetable oils, animal fats and microorganisms. A review of the research on FFA fractionation via urea complex was given by Hayes (41). One of the advantages of using urea complexes separation is that it can also protect the unsaturated fatty acids from oxidation.

Iverson *et al.* (30) fractionated lanolin acids by urea. The 15 fractions he obtained gave the evidence of a preferential complexing order of saturated > branched (*iso* and *anteiso*) > hydroxyl acids. The introduction of methyl group (*iso* or *anteiso*) reduced the binding ability of saturated, unbranched acids equivalent to 2-4 carbon atoms reduction of chain length, whereas a hydroxyl group decrease binding equivalent to 6 carbon atoms of chain length.

Based on the differential binding of FFA with urea, Sumerwell (42) developed a discontinuous liquid-solid counter-current distribution procedure for separating mixtures of fatty acids. After an equilibration among urea, methanol and FFAs, those FFAs less likely to form complexes dissolved in the solvent, and served as the mobile phase while the precipitates of urea complexes served as the stationary phase. When the liquid phase was moved to a fresh tube containing urea, saturated methanol solution with urea was added to the original tube. This procedure was repeated over 10-20 tubes. The distribution of FFAs between mobile phase and stationary phase depended on their molecular structure, following the general complexation rule described previously. This procedure was effective to separate saturated acids from unsatuarated acids, *cis-trans* isomers, and polyunsaturated acids.

Materials and Methods

Chemicals and reagents

All solvents and general chemicals were bought from Fisher (Pittsburgh, PA). Anhydrous lanolin, cholesterol standard, and aluminum oxide (surface area ~155 m^2/g) were purchased from Sigma-Aldrich, Inc, (St. Louis, MO). A standard mixture of normal chain fatty acid methyl ester (FAME) was purchased from Nu chek Prep, (Elysian, MN). TLC plates, used for separating polar lipids, were bought from Analtech (Newark, DE) with 250 μM silica gel as stationary phase.

Measurement of saponification number

In order to obtain good saponification and extraction on large scale, it was important to keep appropriate reactants ratios. The saponification number was determined to qualify the optimum reaction condition.

The alcoholic alkali solution for saponification was prepared by dissolving 3.46 g sodium hydroxide in 90 ml of ethanol and 10 ml of CO_2-free water. About 3.67 g melted lanolin and 10 ml alcoholic sodium hydroxide was mixed in a test tube with a rubber stopper connecting to an air condenser. The test tube was heated over a naked flame with rigorous shaking until all the reagents mixed well and gently boiled. Then the test tube was placed onto a steam bath and heated for 40 min. A warm mixture of 50 ml ethanol, 3 drops of phenolthelein indicator, and 25 ml 0.1N HCl standard solution was added after saponification to dilute the saponification product. The 25 ml HCl was determined from preliminary tests to be less than the amount needed for neutralization. Duplicated titration with 0.1N HCl was done following AOCS Official Method Cd 3-25.

Saponification of lanolin and removal of unsaponifiables

The procedure of saponification and extraction of unsapoifiables generally followed Barn *et al*'s procedure (32). About 33 g lanolin was melted and mixed with 100 ml of warm alcoholic alkali solution in a preheated refluxing flask. The mixture was rapidly heated to boiling and refluxed for 40 min with stirring.

Next, 170 ml warm water (70°C) was added to the saponification mixture and the unsaponifiables were removed by repeated extraction with warm heptane (70°C). At least seven extractions were necessary for complete extraction. During extraction, the funnel was kept at 70°C. A rubber stopper with a one-meter air condenser tube was used at the top of the funnel for condensing any evaporated alcohol. The aqueous layer, which contained mostly the sodium soap of lanolin fatty acids, was treated with 150 ml of 10% (w/v) aqueous calcium chloride solution on a steam bath for 4 hr. After most of the ethanol was evaporated, the granulated calcium soaps were dried, powdered, filtered on a Buchner funnel, and washed twice with distilled water. The dried yellow powder weighed ~20 g.

Methylation of lanolin fatty acids

The 20 g calcium salts were converted to methyl ester with concentrated sulfuric acid (6 ml), methanol (300 ml), and benzene (300 ml) following the procedure of Downing *et al* (29). The mixture was refluxed for about 4 hours. After filtration on a Buchner funnel, the cloudy liquid was centrifuged. Two extractions with water were done to remove the acid and excess methanol from the benzene solution of methyl esters. The benzene solution was evaporated on a rotary evaporator. Typically, 15 g methyl esters of lanolin acids were obtained.

Identification by gas chromatography (GC)

The methyl esters were analyzed by a direct injection on a HP 5890 Series II Gas Chromatography (Heweltt-Packer Company, PA) with a SPB-5 fused silica column (30 m*0.25 mm *0.25 μm, Supelco, PA). The injector and flame ionization detector were set at 300°C. The oven temperature was programmed from 100°C to 300°C at a rate of 10°C/min. The flow rates of hydrogen, helium, air, split and septum purge were set at 29.3 ml/min, 30 ml/min, 316 ml/min, 130 ml/min, 3.4 ml/min. One microliter samples were injected. Chromatographic peaks of saturated FAME were identified by comparing the retention time of (a) a C10:0 to C18:0 normal chain FAME standard or (b) a C17:0 FAME standard. The peaks of unsaturated FAMEs were determined in a same type of GC with a SP-2330 fused silica column (15 m*0.25 mm *0.20 μm, Supelco, PA). The cholesterol peak was identified with a commercial standard. The tentative identification of branched FAME was according to the chromatograph characteristics reported by Pelick and Shigley (31).

Purification by alumina adsorption chromatography

Methyl esters (15 g) were dissolved in a hexane: diethyl ether (94:6) mixture and added to a column containing 100 g of activated alumina. The esters were eluted with the same solvent and yielded 5 g purified methyl esters. The resulting methyl esters were examined by thin-layer chromatography developed with hexane/diethyl ether/acetic acid of 80:20:1. The separated spots were visualized by spraying 0.01% (w/v) dichlorofluorescein in methanol. The esters were also examined by GC. By repeating the procedure above, 44g purified methyl esters freed from hydroxyl compounds were collected. The polar compounds were eluted from the column by acetone and/or methanol.

Spinning band distillation

The methyl esters purified by alumina adsorption were separated by vacuum distillation through a B/R spinning band distillation system (B/R Instrument Corporation, U.S.A.), which has considerably less column hold-up than the still available to Weitkamp. A pot flask filled with FAME was connected to the bottom of the column. A magnetic stir bar was used to obtain an even heating effect. To prevent heat loss, the distillation column was coated with a heating tape to control the surface temperature of the column to be close to the boiling point of the fractions. The pot flask was treated in the same way. The receiver and each joint were connected tightly and the thermometers in the pot flask and in the distillation head were lubricated with high vacuum grease. The power level for proper heating of the pot flask was set and the pressure of the distillation was kept at 0.8 mmHg. Once sufficient heat was generated to boil the contents, vapors began to rise through the distillation column. When vapor reached the condenser, the spinning band was started. After equilibration for a long time (usually 7-8 hr) and continuously raising the pot temperature up to 180°C, liquid began to condense in the still head and was collected in receivers. The head temperature varied during collecting. We kept raising the pot temperature until it reached 260°C. Two distillations were done, and 18 fractions were collected. Then each fraction was treated individually by counter-current urea crystallization.

Counter-current distribution of methyl esters with urea

Distribution system formation

Solutions of urea in methanol at concentrations of 0.049 g/ml, 0.116 g/ml, and 0.150 g/ml were prepared in sufficient amount and stored at room temperature (~20˚C). We named

these three prepared solutions as “40% saturated urea”, “50% saturated urea”, and “65% saturated urea”, respectively.

The distribution was accomplished in a series of 50-ml test tubes, each of which contained 0.4 g pure urea, except for tube 1. About 1 g methyl esters from a distillation fraction and 25 ml 65% saturated urea solution were added to tube 1. A certain amount of urea enough to form complexes with the individual methyl esters that we expected to be kept in the solid phase was also added to tube 1. The amount of urea added was calculated as follows with distillation fraction #19 as an example.

In fraction #19, there were 70.4% of C16i, 2.76% of C16:1, 5.59% of C16:0, 12.44% of C15a, 6.97% of C15:0, 0.63% of C15i, 0.3% of C14:0, and 0.68% of C14i. About 1 g start material was used. The goal of the experiment was to leave normal chain components in the solid phase. Thus, the needed urea for each component was calculated by multiply the coefficient listed in Appendix:

1g FAME * 70.4% C16i * 3.06 = 2.15 g
1g FAME * 5.59% C16:0 * 3.06 = 0.17 g
1g FAME * 6.97% C15:0 * 3.04 = 0.21 g
1g FAME * 0.63% C15i * 3.04 = 0.02 g
1g FAME * 0.3% C14:0 * 3.02 = 0.01 g
1g FAME * 0.68% C14i * 3.02 = 0.02 g
Σ = 2.58 g (urea needed for first tube)

The numerical coefficient is the amount of urea needed to form a complex with 1 g of a certain chain length of the FAME indicated.

After being well sealed with a Teflon tape and screw cap, the tube was heated in a 60°C water bath until all the urea and methyl esters melted and dissolved in the solution. A magnetic stir bar was used to assist rapid solution and even crystallization. The tube was then

allowed to cool to room temperature with stirring and left for at least two hours to reach equilibrium between the solid and liquid phase.

The liquid portion in tube 1 was transferred to tube 2, and 25 ml of 50% saturated urea solution was added to tube 1. If the urea complex was well-formed large crystals, the liquid could be directly decanted. If the crystals of complex were extremely fine, a 10-ml Luer syringe with a 15 cm blunt-end needle (20 Gauge) would be used to remove the liquid to avoid carrying crystals to the succeeding tube. The mixtures in both tube 1 and tube 2 were heated on water bath to achieve solution, and cooled to room temperature. The liquid in tube 2 was transferred to tube 3, the liquid in tube 1 to tube 2, and 25 ml 50% or 40% saturated urea solution was added to tube 1. The addition of saturated urea solution depended on how well the crystal formed in tube 1, and will be discussed in results. The transfer process was repeated until the methyl esters were distributed over 10 to 15 tubes. The precipitates of adducts were usually well formed. If not, rigorous shaking, suddenly blowing air to the surface by using an empty syringe, or temporary cooling (-8˚C), would be used to induce crystals.

Urea complex decomposition and GC analysis

Once tube 1 was observed not to form crystal easily, a 1-ml sample was taken from the liquid phase of the first tube and last tube separately to determine if the distribution was enough to separate the components. These samples were treated with 10 ml hot water (60˚C), 3 drops of concentrated hydrochloric acid and 1 ml hexane. Then 1 µl of the hexane extract was injected into GC.

If the distribution seemed finished (based on analysis of the composition of the first and last tube; see results for an example), the liquid in each tube was transferred to a 125-ml

erlenmeyer flask. The addition of 100 ml hot water (60°C) and 2 ml of concentrated hydrochloric acid decomposed the complex and release the methyl esters. The solids left in the test tube were treated as the same way as the liquid with the addition of 40 ml of hot water (60˚C) and 1 ml of concentrated hydrochloric acid. Then the methyl esters were recovered by extraction with hexane or diethyl ether. Since short chain methyl esters (carbon number less than 14) were quite volatile, they were extracted with diethyl ether to reduce the loss during solvent removal. The methyl esters obtained separately from the solids and liquids of each tube in the counter-current distribution were examined by GC. Samples having similar compositions by GC% were combined.

Low temperature solvent crystallization

Crystallization in the freezer (-18˚C)

About 250 mg methyl ester from distillation fraction #9 was dissolved in 5 ml acetone. Then the 5% (w/v) acetone solution was put in a -18ºC freezer for 3 hr equilibration. Filtration was done in the freezer with a sintered glass tube filter at the same temperature to obtain the first filtrate (9f1). A small amount of acetone (~2ml) was used to wash the filter and the washing liquid was combined with the precipitates. After another 3 hr equilibration, a second filtration was done and a second filtrate (9f2) was obtained. By repeating same procedure, a third filtration gave the third filtrate (9f3) and a precipitate (9p). Other distillation fractions were treated as the same way, but in various solvents (hexane, acetone, or methanol) with limited success.

Crystallization in a solid carbon dioxide-acetone bath

About 100 mg *ante*-C17 sample at 85% purity obtained from urea counter-current

distribution fractions was subjected to low-temperature crystallization. About 5 ml ethyl acetate was used to make a 2% (w/v) solution. The diluted sample was put into the dry ice-acetone bath, and slowly cooled down with constant shaking. The temperature of the bath was controlled by adding dry ice. After equilibration at -73˚C for about 20 min, we used a -73˚C sintered glass tube filter connecting to a syringe to suck the liquid out. The precipitate was dissolved in another 5 ml of ethyl acetate and heated until all crystals dissolved in the solvent. Again, the mixture was slowly cooled down to -73˚C and filtrated. The same procedure was repeated three more times. Altogether, four filtrates and one precipitate were obtained. The sequence of crystallization and filtration is given in Fig. 3. During the filtration, the addition of the 5 ml portions solvent added after each separation to the precipitate, was firstly used to wash the filter and then combined with the precipitate. The filtrate and precipitates were analyzed separately by GC. After GC analysis, 1 g sodium sulfate was added to the samples to absorb the moisture accumulated during filtration. A microfilter was used to remove sodium sulfate. The ethyl acetate was evaporated under a stream of nitrogen gas until the weight of the sample did not change. A sample of *ante*-C15 (~80% purity) was used in a preliminary test with ethyl acetate as crystallization solvent. The filtrations were at successively lower temperatures to find the ideal crystallization point. The details were given in the results section. A sample of *ante*-C13 (~80% purity) was crystallized in the same procedure as *ante*-C17. The crystallization solvent used for *ante*-C13 was acetone instead of ethyl acetate since shorter chain esters are more polar.

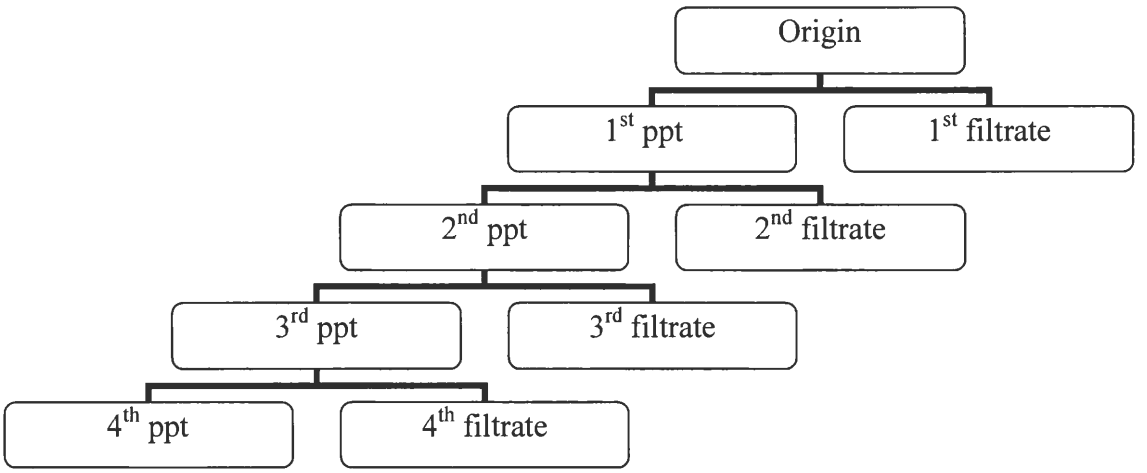

Fig. 3. Flowchart of dry ice-acetone bath crystallization

Preparing isopropyl ester from branched-chain methyl esters

For easy preparation of catalyst of the transesterification, we added extra isopropyl alcohol to 1 N sodium isopropoxide to make a 1% (w/v) alcoholic sodium isopropoxide. To do this, 40-50 mg sodium metal was reacted with 100 ml isopropanol. The reaction flask was connected to a dryrite/soda lime filter to keep the moisture and CO_2 away and let the hydrogen gas out. Transesterification was achieved by mixing methyl ester and the diluted catalyst with rigorous stirring at room temperature for 3 hrs. The molar ratio of methyl ester and isopropanol in the reaction was about 1:200. About 15 ml alcoholic catalyst was added to 50 mg methyl ester. Upon the completion of reaction, a small amount of acetic acid was added to neutralize the catalyst, and the isopropyl ester was extracted with hexane.. The excess isopropanol and acetic acid were washed away with 5% (w/v) sodium bicarbonate. The hexane was evaporated under nitrogen gas. The isopropyl esters were analyzed with GC. Before we transesterified branched-chain methyl esters, normal chain C12 and C18 FAME

(99% pure) were used to examine the optimal reaction conditions. The C12 FAME was prepared in our lab. The C18 FAME was from a commercial source.

Using DSC to measure melting points and heats of fusion of methyl esters and isopropyl esters

The melting point and heat of fusion of individual branched-chain methyl esters and isopropyl esters were measured by a differential scanning calorimeter (DSC7) equipped with Intracooler System II (Perkin Elmer, Norwalk, CT). Indium and *n*-decane were used to calibrate the equipment. About 5-7 mg samples were weighed accurately into stainless steel pans and an empty pan was used as a reference. The sample and the reference were rapidly heated from 25°C to 80° at 40°C/min to completely melt the sample, held for 10 min, and then the sample was cooled to -80°C at 10°C/min. The cooling rate affects the crystallization onset temperature but not the melting point, and 10°C/min was recommended by the AOCS Official Method Cj 1-94. The sample was held isothermally for 15 min at -80°C, and reheated to 80°C at 5°C/min which was reported to be the ideal heating rate when measuring isopropyl esters (9). The above temperature program is called the standard temperature program in the discussion section. Replicates (≥2) were performed on each sample. The calorimetric parameters obtained from heat flow (mW) vs. temperature (°C) curves in the melting scan were melting onset temperature (T_{on}), temperature of the completion of melting (T_{com}), temperature of maximum heat flow (T_p), and heat of fusion (ΔH).

Using ^{13}C NMR and ^{1}H NMR to verify the molecular structures of branched-chain esters

The molecular structures of the branched-chain esters were examined by ^{13}C NMR and ^{1}H NMR, except for *ante*-C13-ME, *ante*-C17-ME and *iso*-C18-IE because of the lack of materials. The ^{13}C NMR spectra were measured with a Varian VXR-400 NMR spectrometer. The ^{1}H NMR spectra were measured with a Varian VXR-300 NMR spectrometer. A Heteronuclear Multiple Quantum Correlation (HMQC) experiment was done on a Bruker DRX-400 NMR Spectrometer to determine which hydrogen of a molecule are bonded to which carbon nuclei. A small amount of the ester was dissolved in 0.6 ml $CDCl_3$ and 5 mm NMR tubes (Kontes Glass Co. Vineland, NY) were used. For the ^{13}C NMR spectra, the assignment of chemical shifts of important carbon atoms of the esters was done with ACD/ChemSketch Predictor software from Advanced Chemistry Development Inc. (Toronto, Ontario, Canada).

Results and discussion

Preparation of methyl esters

During extraction, it was necessary to keep the mixture at 70°C. Otherwise, the saponifiables and unsaponifiables would remix and precipitate, and make the extraction impossible. We used a self-made water bath having the same height as the 1000-ml separatory funnel used for extraction to keep the mixture warm. Another critical operation was to keep water and ethanol ratio at 2:1. This was accomplished by using long glass tube functioning as an ethanol condenser instead of a glass stopper for the funnel. We also tried to avoid the formation of the three liquid layers since this event would lower the extraction yield. If three layers formed, a small amount of ethanol was added to adjust the ratio of ethanol/water.

At the beginning of our saponification experiment, we could hardly get more than a 50% yield using the reactant ratio of Barnes *et al* (32). The lanolin we purchased was slightly different from the wool wax that Barnes *et al.* used fifty years ago. We measured the saponification number to identify the type of lanolin and examine the amount of excess alkali. Its saponification number was 91. From the saponification number we calculated the excess sodium hydroxide left after the saponification to be between 68-70%. We reduced the amount of alkali added at the beginning of saponification to achieve the desired level that gave us 50% excess alkali as Barnes *et al.* suggested. By changing the amount of excess alkali and controlling the extraction temperature and ratio of ethanol/water, we were able to improve our yield by 10-20%.

The methyl esters of lanolin acids were a yellow mixture and solid at room temperature. They included more than 100 compounds as shown in Fig. 4a.

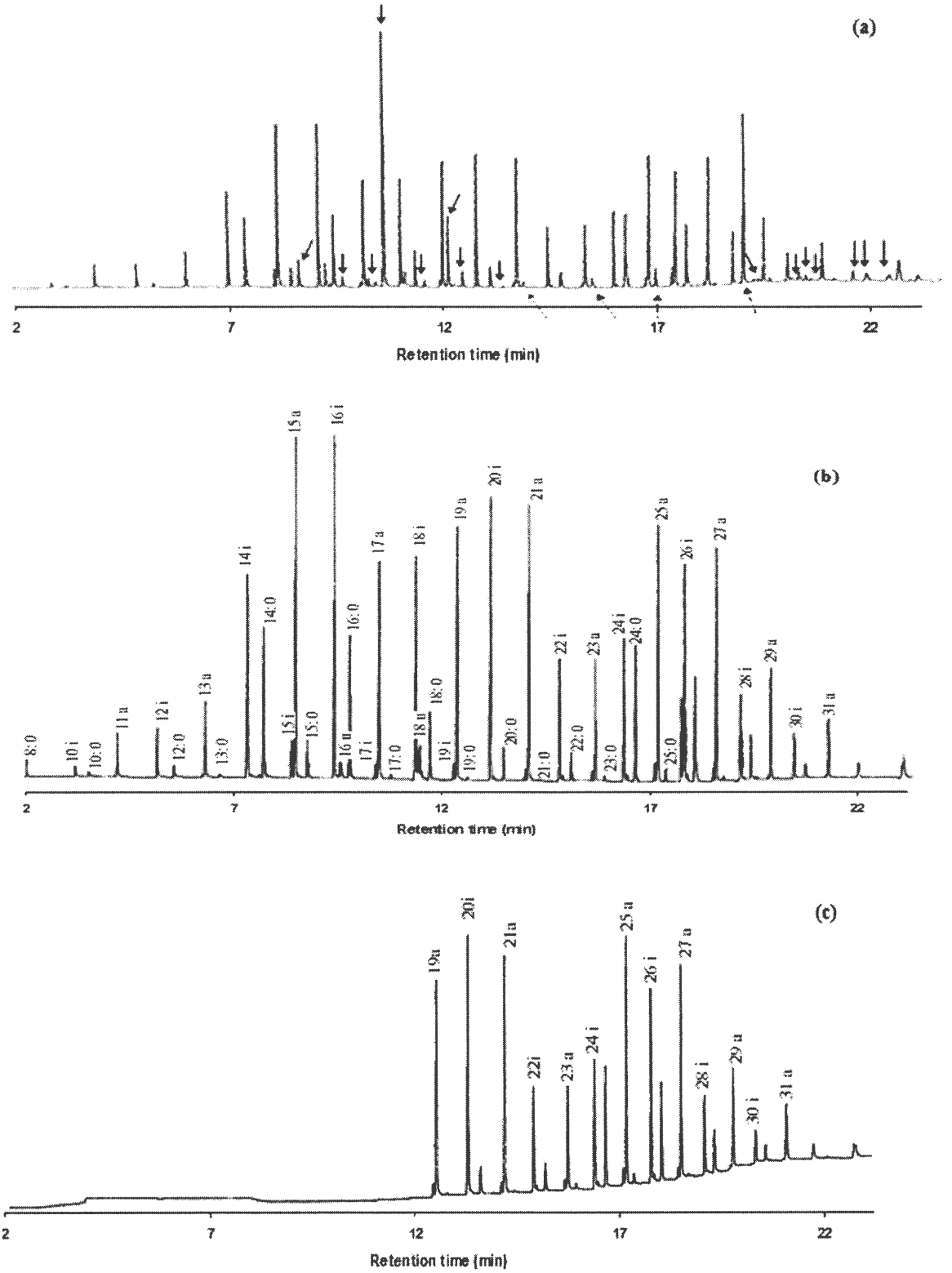

Fig. 4. Gas chromatography of lanolin fatty acid methyl esters of a) after methylation b) after alumina adsorption c) pot residual after distillation

Removal of polar impurities and tentative identification of methyl esters

The alumina column adsorbs the polar lipids and lets the non-polar compounds run through. In this way, we removed most of the polar compounds. The first product of alumina separation did not give the polar band on a thin-layer plate that was detected before the column purification. This means that we removed most of the hydroxy acid with the alumina column. The peaks marked with solid arrows and dashed arrows in Fig. 4a were those that were completely removed and those had reduced amount after alumina column purification. The polar compounds had a yellow color when eluted from the alumina with polar solvents. By comparing our GC to Pelick and Shigley's GC result and normal chain standards, we tentatively identified the *iso*- and *anteiso*- branched chain and normal chain FAME with chain length 10 to 31 as shown in Fig. 4b, following Pelick and Shigley's rule that "*iso*- compounds almost always give a smaller peak in company with the normal even carbon acids whereas the *anteiso*- compounds show just the opposite in company with the odd carbon acids" (31). There were usually some small peaks coming out right before the *anteiso*- compounds with very small time interval (0.1 min) on GC graph, such as the peak shown before *ante*-C15, *ante*-C17 and *ante*-C19 (Fig. 4b). They were tentatively identified as the corresponding *iso*- odd chain FAMEs. Pelick and Shigley also found these peaks and suggested that they might be odd chain *iso*- compounds (31). Since we did not have any standards or earlier research identifying these components and we were not able to isolate these trace components in this experiment, we could not be completely sure about this conclusion, although the behavior of those components in the counter-current urea separation supported this conclusion.

Since the major goal of this project was to investigate the melting characteristics of branched chain fatty acids, we did not analyze the polar compounds eluted by methanol/acetone, which probably contain large amounts of hydroxy compounds. Considering that hydroxy fatty acids are used in a wide range of products, including cosmetics, coatings, resins, etc., it will be valuable to know if isolating hydroxy fatty acids from the adsorbed substances is feasible and economic.

Spinning band distillation

Since the column head temperature indicator on the control panel of microprocessor controller did not correspond to the real vapor temperature very well, we were not able to collect the fractions by the boiling point, which is critical for optimum separation. The reason why the temperature indicator did not function as expected is uncertain. The blind fraction collecting we were forced to use resulted in the fractions having broad ranges of chain length. The head temperature measuring the vapor temperature when it reached the condenser, was observed to increase from 20°C to 63°C with intervals, and then gradually dropped back to 40°C. This was repeated with each higher boiling fraction until the distillation finished. The basic criterion to collect the fractions in our case was to take new fraction at the start of each rising temperature. The true boiling temperature is expected to be in the range of 60-160˚C at pressure we used (43). Possibly the low values were caused by poor heat transfer to the thermal-couple and the low heat capacity of the boiling vapors at 0.8 mmHg.

Another limitation was the maximum temperature we could reach. Based on the equipment capability of our lab, we could not reach a higher temperature than that needed for C18 group. Most of the branched long chain FAMEs (chain length larger than 19) were left as the pot residue as shown in Fig. 4c.

The first and second distillations gave ten fractions and eight fractions, respectively, each of which was a mixture of branched and normal chain FAME. The major components of each fraction differed by 1 or 2 carbon numbers. In Table 2, fractions #1 to #12 were from first distillation, and #13 to #20 were from second distillation. The major components in each fraction are printed in bold type. Fractions #5, #6, #8, and #9 were most abundant fractions by weight.

The distillation results were not as good as expected. The fraction with highest purity was # 16 which consisted of 86% *iso*-C14. The major impurities were C14:0, C13:0, and *anteiso*-C13. The chain lengths of components in our best fraction varied from 11 to 14. The worst fraction consisted of more than 20 components in addition to the major component, and caused a great deal of trouble in crystallization.

Counter-current distribution of methyl esters with urea

Using unsaturated urea-methanol solution instead of completely saturated solution

In the preliminary tests of urea counter-current distribution, we used same ratio of FAME/urea as Sumerwell used (42), and a saturated urea-methanol solution for the liquid phase. But the results showed that saturated urea-methanol hardly took any FAMEs from the solid phase of first tube to the mobile phase of next tube. This problem was solved by using less saturated urea-methanol solution to keep the compounds less able to form a complex with urea into the liquid phase. Once unsaturated urea-methanol solution was added to the solid complex, part of the urea in the complex would dissolve in the new added solution. Having less available urea led to a competition among the FAME components to form urea complexes. Those compounds easy forming complex with urea, such as saturated normal and

Table 2. FAME profile of distillation fractions by GC (%)

	#1	#2	#3	#4	#5	#6	#8	#9	#11	#12	#13	#14	#15	#16	#17	#18	#19	#20
9a	0.4	0.1									0.3							
9:0	0.7	0.2			0.1						0.4	0.1						
10i	**20.6**	3.9	0.4	0.1	0.4						**8.2**	2.3	1.0					
10:0	**24.8**	3.4	0.4								**11.9**	2.9	1.1					
11i	2.9	0.8	0.1								1.4	0.6	0.2					
11a	**44.4**	**24.7**	2.3	0.5							**35.2**	**15.7**	4.3	0.3		0.3		0.2
11:0	0.2	4.3	0.3								1.6	1.5	0.3					
12i		**59.4**	**21.5**	1.7	0.3						**21.9**	**54.7**	**9.9**	0.7		0.4		0.5
12a		1.0	0.6								0.3	1.0	0.5					
12:0		0.6	**26.1**	1.2	0.1						0.8	**18.7**	**10.3**	0.3		0.2		0.2
13i			3.3	1.3							0.1	0.2	4.1	0.2				
13a			**43.7**	**25.2**	0.6	0.1		0.0			0.7	1.8	**62.4**	**6.3**	1.0	1.7	0.2	1.0
13:0			0.4	3.7	0.1								3.2	2.1	0.2	0.2		0.2
14i				**52.3**	**18.6**	0.3	0.1	0.1			1.1		2.2	**85.7**	**19.3**	3.0	0.7	1.4
14:0				12.5	**23.5**	0.5	0.1	0.1			1.1			3.0	**29.2**	3.1	0.3	0.7
15i					5.8	1.7	0.1				0.3				5.9	**6.3**	0.6	0.5
15a					**47.6**	**21.0**	0.9	0.3			2.0				**40.8**	**80.5**	**12.4**	**7.8**
15:0					1.8	9.6	0.5	0.1			0.3				0.7	2.7	7.0	2.3
16i						**53.8**	**49.8**	3.7	0.2	0.6	2.2				0.9	1.6	**70.4**	**70.8**
16:1						3.8	5.9	0.6			0.3						2.8	5.0
16:0						8.8	**31.7**	5.4	0.2	0.6	1.6						5.6	**9.2**
17i							0.4	3.2	0.1	0.1	0.2							
17a						0.1	3.5	**44.2**	1.4	1.5	2.4							
17:0								1.7	0.1	0.1	0.1							
18i								**27.7**	**57.1**	**24.3**	2.4							
18:1								2.1	6.8	3.5	0.8							
18:0								1.7	**28.0**	**58.8**	1.4							
19a									0.5	0.1								
Weight (g)	0.36	0.41	0.55	1.60	5.01	2.90	2.70	4.01	1.37	0.40	0.29	0.15	0.34	0.40	0.65	0.40	1.47	0.09

long chain FAME would win the urea in the competition and form crystals and stay in the solid phase. Inevitably, some of these compounds would not get enough material when the amount of urea is limited, and thus enter the liquid phase of next tube. Therefore, it was necessary to make up of a certain amount of urea to next tube to retain those compounds. What happened in the next tube was similar to the previous tube that all components competed for limited urea to form complex.

Preparation of urea-methanol solution

The concentration of saturated urea-methanol solution was 1 g/6 ml in the Merck Index. In our experiment, 1 g urea would dissolve in 4.3 ml methanol to reach saturation. Considering the difference existing in lab conditions and materials, we prepared urea-methanol solution based on our data. Therefore, we had a 40% saturated urea" solution at 0.049g/ml, "50% saturated urea" solution at 0.116g/ml, and "65% saturated urea" solution as 0.150g/ml.

Determination of the end point of distribution

After analyzing samples by GC, we could have an approximate estimation of the distribution. Taking distillation fraction #11 as an example, the major component was *iso*-C18, and major impurities were C18:0 and *ante*-C17 (Table 3). According to the expectations of the compounds' capability of forming complexes, we supposed that C18:0 and C16:0 stayed at the first few tubes, C18:1, and some short chain esters stayed in the last few tubes, *iso*-C18 and *ante*-C17 stay in the middle tubes. The distribution scheme of the components was supposed to be like this:

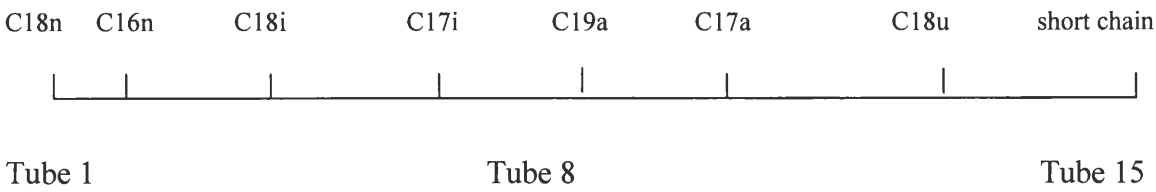

n = normal, u = unsaturated (one double bond), i = *iso*, a = *anteiso*

If the first tube consisted mostly of the normal chain group and last tube contained some short chain group or perhaps a small amount of C18:1 or C17a, we would stop the distribution and break the complex to recover the products.

Determination of the addition of specific urea-methanol solution

Since we kept adding urea-methanol solution to tube 1, we had to decide what concentration would be needed to release an appropriate amount of components from the solid phase of tube 1 to tube 2. The concentration of the solution to be used depended on how much crystal formed in tube 1. Basically, if there were too much urea in tube 1, most of the components would form a complex (we would see lots of crystals.) and we would need more methanol to dissolve the "excess" urea in order to provide a desired competitive environment of complex formation; therefore, a less saturated solution would be used, i.e. 50% saturated urea. The 40% saturated urea was used cautiously because excess methanol would prevent the solid phase interacting with easily-complexing esters and therefore weaken the effectiveness of the counter-current system. We used 40% saturated urea only when the crystals in tube 1 were not observed to decrease and the next tube hardly formed crystals with the addition of pure urea.

Preferential order for urea complexing

With the modified urea counter-current distribution, we obtained 95% pure *iso*-C18 from distillation fraction # 11, 98% pure *iso*-C16 from fraction #19, 95% pure *iso*-C14 from fraction #4, 88% pure *ante*-C17 from fraction #9, 95% pure *ante*-C15 from fraction #18, and 80% pure *ante*-C13 from fraction #15 as shown in Table 3~8. In general, the ease of forming urea complexes was: normal C_{n+1} > normal C_n > normal C_{n-1} > *iso*-C_n > unsaturated C_n > *anteiso*-C_{n-1} (where n is a particular chain length). This was indicated by the tube in which the highest purity of each individual ester peaked. As shown in Table 3-13, the percentage in bold type indicates in which tube/fraction the highest purity of each components resides. If the highest purity appeared in an early fraction, it means that compound formed complexes with urea easily. The compounds that accumulated in the last tube formed urea complex with difficulty. So, Table 3 showed an order of ease of forming urea complexes as C18n > C18i > C19a > C17i > C18u & C17a. Other trials showed C15n & C16n > C16i > C15i & C16u > C14i > C15a > C13a (Table 4), C14n > C13n > C12n > C14i > C13i > C13a &C12i (Table 6), C18i & C17n & C16n > C17i > C16i > C18u > C16u & C17a (Table 7), C15n > C16i & C14n & C13n > C15i > C14i > C15a > C13a (Table 8), C13n > C12n > C14i > C10n > C12i & C13i > C13a > C11a (Table 9), C12n > C11n > C10n > C12i > C13a > C10i & C11a (Table 10). The solid phase kept all components in the same order as the liquid phase, but the maximum peak appeared later in solid phase than in liquid phase as shown in Table 4 and 5.

Table 3. Composition (GC %) of the liquid phase of urea countercurrent distribution of distillation fraction 11

ME / Tube #	17i	17a	18i	18:1	18:0	19a
start	0.2	2.3	57.6	6.1	28.3	0.6
1	0.1	-	89.7	-	***8.9***	0.4
2	0.1	-	95.7	-	2.8	0.6
3	0.1	-	***96.4***	0.1	1.2	0.9
4	-	-	96.1	0.6	1.4	-
5	-	-	92.9	1.9	0.6	-
6	0.3	0.4	94.5	2.5	0.4	-
7	0.3	0.5	91.9	3.4	0.3	***1.5***
8	***0.5***	1.0	90.2	5.4	-	-
9	0.3	0.8	90.0	5.8	0.1	-
10	-	***6.8***	37.2	***42.3***	-	-

Table 4. Composition (GC %) of the liquid phase of urea countercurrent distribution of distillation fraction 19

ME / Tube #	13a	14i	15i	15a	15:0	16i	16:1	16:0
start	0.4	0.7	0.7	12.5	7.57	65.03	3.9	7.1
1	-	-	-	-	***40.8***	27.6	-	***29.3***
2	-	-	-	-	20.5	69.9	-	7.1
3	-	-	0.1	-	10.2	85.3	-	1.8
4	-	-	0.2	-	1.5	97.1	-	0.1
5	-	-	0.4	0.1	0.4	***98.3***	0.1	-
6	-	0.2	1.1	0.7	-	95.1	2.0	-
7	-	0.3	1.2	2.0	0.1	92.4	3.1	-
8	-	1.2	1.6	11.8	-	73.9	9.7	-
9	-	2.4	***2.1***	32.9	-	43.5	***16.2***	-
10	0.4	***3.1***	-	66.8	-	10.7	15.5	-
11	2.5	2.6	-	***84.4***	-	0.8	5.9	-
12	4.2	2.5	0.4	76.8	-	2.4	6.9	-
13	***7.5***	1.4	0.5	56.9	-	2.1	4.1	-

Table 5. Composition (GC %) of the solid phase of urea countercurrent distribution of distillation fraction 19

ME / Tube#	13a	14i	15i	15a	15:0	16i	16:1	16:0
start	0.4	0.7	0.7	12.5	7.6	65.0	3.9	7.1
1	-				36.2	3.6		***58.1***
2					***40.6***	20.4		36.9
3					34.9	48.2	0.4	14.1
4			0.1		8.4	88.2	0.5	1.4
5			0.2	0.02	0.8	***98.2***	0.1	
6			0.5		0.2	***98.2***	0.3	
7		0.1	0.8	0.4		96.6	0.9	
8		0.3	1.3	2.0		91.6	4.0	
9		0.9	***1.9***	9.3		77.8	8.6	
10		2.4	1.9	41.9		30.1	***20.1***	
11	1.9	2.4		***82.1***		1.6	6.1	
12	1.8	***2.8***	0.7	75.1		5.8	11.6	
13	***19.63***			41.50				

Table 6. Composition (GC %) of the liquid phase of urea countercurrent distribution of distillation fraction 4

ME / Tube #	12i	12:0	13i	13a	13:0	14i	14:0
start	1.8	1.4	1.3	25.3	3.9	51.4	12.4
1					3.2		***93.9***
2					12.2	1.9	86.0
3					***26.6***	4.8	68.7
4		***8.4***			25.7	41.7	24.2
5		4.1	0.3		4.8	88.3	2.5
6	0.2	0.9	0.8	1.2	0.3	***96.0***	0.1
7	1.3	0.2	2.3	11.1		83.4	
8	4.0		***2.9***	58.8		29.9	
9	***4.5***		1.5	***84.7***		5.7	
10	3.7		0.7	83.2	0.2	2.3	

Table 7. Composition (GC %) of the liquid phase of urea countercurrent distribution of distillation fraction 9

ME / Tube #	16i	16:1	16:0	17i	17a	17:0	18i	18:1
start	4.5	0.6	6.6	3.1	47.8	2.2	28.5	2.6
1	1.5	-	***13.6***	4.9	3.2	***3.1***	***70.0***	0.3
2	5.6	3.7	3.7	***8.0***	24.2	0.7	54.3	2.4
3	6.3	-	2.8	6.8	34.4	0.5	45.6	2.7
4	***7.1***	-	1.1	5.5	53.9	0.2	26.9	4.3
5	6.9	0.1	-	3.2	71.6	-	12.4	***4.8***
6	5.0	0.4	-	1.0	86.8	-	1.7	4.2
7	5.7	1.0	-	-	85.3	0.6	-	2.0
8	4.6	***1.6***	-	-	***88.4***	-	-	2.1
9	4.5	1.4	-	-	69.2	-	1.1	1.4

Table 8. Composition (GC %) of the liquid phase of urea countercurrent distribution of distillation fraction 18

ME / Tube #	13a	13:0	14i	14:0	15i	15a	15:0	16i
start	1.9	0.3	3.2	3.6	6.5	77.4	3.3	2.0
1	-	1.0	-	33.9	1.1	2.4	***54.2***	4.2
2	-	**2.1**	-	***40.4***	9.2	1.8	30.1	***13.0***
3	-	1.7	3.9	9.1	***34.3***	33.3	3.2	12.7
4	-	0.5	5.7	0.9	14.3	73.6	-	2.8
5	-	-	***4.7***	-	6.2	87.8	-	0.6
6	-	-	3.5	-	2.3	93.3	-	-
7	-	-	2.7	-	0.9	***95.2***	-	-
8	1.4	-	2.0	-	-	95.0	-	-
9	10.1	-	1.4	-	-	83.4	-	-
10	***14.4***	-	1.0	-	-	75.5	-	-

Table 9. Composition (GC %) of the liquid phase of urea countercurrent distribution of distillation fraction 15

ME / Tube #	10:0	11a	12i	12:0	13i	13a	13:0	14i
start	1.5	4.7	10.0	11.0	4.1	59.3	3.5	2.8
1	-	-	1.6	35.7	0.6	9.7	**50.5**	0..66
2	-	-	1.2	***66.1***	0.8	6.8	21.4	2.1
3	3.3	-	4.9	49.8	5.2	19.2	4.8	11.1
4	4.9	-	6.4	32.1	9.4	23.5	0.6	***19.8***
5	***5.6***	-	9.7	17.9	12.1	35.2	-	15.8
6	4.7	-	***14.7***	2.8	***12.9***	55.5	-	7.1
7	1.6	1.5	14.6	-	5.8	73.8	-	1.2
8	-	3.0	11.8	-	2.3	***80.4***	-	-
9	-	10.6	8.0	-	0.6	75.0	-	-
10	-	***23.8***	5.2	-	-	57.6	-	-

Table 10. Composition (GC %) of the liquid phase of urea countercurrent distribution of distillation fraction 14

ME / Tube #	10i	10:0	11a	11:0	12i	12:0	13a
start	2.5	3.2	14.7	1.6	53.5	19.6	2.2
1	-	0.3	-	1.1	0.9	89.2	-
2	-	1.0	-	3.3	2.2	***92.5***	-
3	-	2.9	-	5.8	6.8	83.2	-
4	-	8.6	0.2	***8.9***	22.6	55.9	0.5
5	0.1	***11.4***	0.3	2.9	77.5	4.3	1.52
6	0.2	5.7	0.7	0.8	87.5	1.1	2.5
7	0.7	2.6	3.0	0.2	***88.0***	-0.3	3.4
8	2.6	1.2	12.8	0.1	76.1	-	***3.9***
9	4.5	1.0	23.8	-	61.9	-	3.6
10	7.1	0.8	38.7	0.1	42.9	-	2.6
11	***7.9***	-	***46.7***	-	33.1	-	2.4

Table 11. Composition (GC %) of the liquid phase of urea countercurrent distribution of distillation fraction 5

ME / Tube #	13a	13:0	14i	14:0	15i	15a	15:0
start	0.7	0.1	18.0	23.0	5.9	48.4	2.2
1	-	-	-	***88.6***	-	2.5	***3.7***
2	0.3	1.1	1.7	70.9	9.1	1.7	0.6
3	-	***1.3***	8.3	52.9	***31.6***	4.5	0.3
4	-	0.1	***38.1***	0.6	18.9	41.7	-
5	-	-	33.5	-	5.9	60.1	-
6	-	-	26.0	-	2.1	71.3	-
7	0.2	-	17.5	-	0.3	80.6	-
8	1.1	-	12.2	-	-	***82.9***	-
9	***1.8***	-	13.2	0.1	0.2	80.4	-

Table 12. Composition (GC %) of the liquid phase of urea countercurrent distribution of distillation fraction 6

ME / Tube #	14:0	15i	15a	15:0	16i	16:1	16:0
start	0.6	1.7	20.4	9.8	51.7	4.0	10.1
1	***2.4***	0.1	0.1	***39.1***	33.3	0.2	***24.3***
2	2.0	0.2	-	24.0	62.0	0.2	11.2
3	0.8	0.7	0.1	3.1	94.2	0.1	0.7
4	0.3	1.5	0.4	0.6	***96.1***	0.7	-
5	0.2	3.5	3.4	0.2	87.9	3.9	-
6	0.1	***4.9***	15.4	0.1	68.6	8.9	0.2
7	0.1	4.1	39.6	0.1	40.7	***12.8***	0.3
8	0.1	1.3	82.4	-	4.6	8.5	0.0
9	-	0.5	***87.2***	-	0.9	4.1	0.2
10	-	0.4	67.5	-	0.9	2.3	0.8

Table 13. Composition (GC %) of the liquid phase of urea countercurrent distribution of distillation fraction 8

ME / Tube #	15i	15a	15:0	16i	16:1	16:0	17i	17a
start	0.11	1.22	0.72	51.37	6.34	33.36	0.54	4.76
1	-	-	***3.4***	10.0	-	***82.7***	-	-
2	-	-	2.7	12.4	-	82.7	0.8	-
3	-	-	3.2	23.2	-	71.1	1.3	0.2
4	-	-	2.5	35.1	-	59.4	1.5	0.4
5	-	-	1.8	67.7	-	25.9	***1.9***	1.2
6	-	-	0.6	89.4	-	5.1	1.4	2.8
7	0.1	-	0.1	***91.8***	-	0.5	0.7	5.5
8	0.3	0.3	-	79.0	8.2	-	0.2	11.0
9	1.2	2.2	-	51.5	29.6	-	-	***11.8***
10	0.7	3.9	-	39.0	39.9	-	-	11.5
11	***4.4***	***5.0***	-	33.4	***43.6***	-	-	11.1

In the experiments, we found that the urea-complexing ability of the tentatively identified odd chain *iso*-compounds was between those of its shorter and longer even chain length *iso*-compounds. The results agreed with our expectations based on urea complexing theory and confirmed that the compounds probably were odd chain *iso*-compounds.

Some of the trials did not show a preference between a few components having similar structures, such as normal chain C16:0 and C15:0 in Table 4, 12 and 13. These always occurred in the first two or three tubes where the compounds had remained complexed and were not subjected to much distribution.

The purity of individual methyl ester obtained depended on the composition of the starting materials. A higher percentage of a compound in the starting material (≥50%) was more likely to produce pure products. In addition, a mixture of *iso*-C_n and *anteiso*-C_{n-1} was easier to separate than a mixture of *iso*-C_n and *anteiso*-C_{n+1}. As shown in Table 11 and 8,

fractions #5 and #18 had very different starting materials; fraction # 18 contained 29% more *anteiso*-C15 than fraction #16, although the two fractions contained similar impurities. We were able to get 95% *anteiso*-C15 from fraction #18, but only 83% from fraction #5. Table 12 and 13 showed that fractions #6 and #8 were both rich in *iso*-C16 with similar percentage. The major impurities of #6 and #8 were *anteiso*-C15 and C16:0, respectively. According to the rule of the ease of forming urea complexes, these two impurities should be easy to remove from the *iso*-C16. But, fraction #8 also contained a small amount of *anteiso*-C17 which was very difficult to separate from *iso*-C16 because their tendency to form urea complex was close. As a result, *iso*-C16 of only 91% purity was obtained in fraction #8.

Counter-current distribution of methyl esters with urea proved to be an effective method to isolate highly pure branched chain esters. Moreover, it is a low cost procedure, and the reagents, urea and methanol, can both be recycled. The disadvantage is that its operation was tedious and time-consuming.

Since the amount of branched methyl esters available for urea complexing was not great, each trial was conducted on a 1g scale or less. Further investigation will be needed to examine the effectiveness of large scale separation of branched chain acids with the urea crystallization system.

Low temperature crystallization

Crystallization at -18˚C

The crystallization of distillation fraction #9 from acetone was the most successful example of this method. The major components in this fraction were 44% of *anteiso*-C17 and 28% *iso*-C18. The precipitates contained ~95% of *iso*-C18. The *anteiso*-C17 and other minor components stayed mostly in the filtrates (Table 14). Other trials involving having shorter

chain length did not separate as well as #9 or did not crystallize at all, the esters being too soluble in hexane to crystallize at -18˚C. Using more polar solvents, such as acetone and methanol, resulted in the ester not being soluble at room temperature or separating as a liquid from the cold solvent at low temperature rather than as crystals. These outcomes were observed when we tried to crystallize fractions #12 and # 5.

The disadvantage of this method was that the whole process had to be done in the freezer at -18˚C which was not a comfortable temperature for the operator. Also, we could not control the temperature freely so we only had one crystallization temperature.

Table 14. Solvent Crystallization (GC %) of fraction #9 in dry ice-acetone bath

	16 i	**16 : 0**	**17i**	**17 a**	**17 : 0**	**18 i**	**18 : 1**	**18 : 0**
start	3.7	5.4	3.2	44.2	1.7	27.7	2.1	1.7
9f1	5.3	6.9	4.4	62.7	1.6	11.0	3.1	1.8
9f2	2.7	6.9	2.9	35.9	3.6	44.3	-	3.4
9f3	1.1	3.0	1.1	13.0	2.8	79.0	-	-
9ppt	-	0.8	-	1.3	1.5	***95.5***	-	1.0

Crystallization in solid carbon dioxide (dry ice)-acetone bath

By using the counter-current urea system, we were able to get most of even chain branched methyl esters except *iso*-C12 to >95% purity. For odd chain esters, such as *anteiso*-C17, we could obtain only 82% purity, probably because the *anteiso*-C17 and impurities had the same tendency to form urea complexes at the concentrations in which they occurred.

Preliminary tests of crystallization of ante-C15 and ante-C17

ante-C15 (~80% purity) from the combined fractions of the urea countercurrent system was used in this dry ice-acetone crystallization. As a preliminary experiment, two filtrations were done at –50ºC and –55ºC on a 5% solution of ethyl acetate, and gave first (1st

ppt) and second precipitates (2nd ppt) with 88% and 86% purity, respectively. The filtrate (2nd filtrate) was rich in *iso*-C14. After combining the two precipitates, another three filtrations were done at –45°C, -60°C and –75°C. The highest purity ~90% appeared in the fourth and fifth precipitates (Fig. 5). Ninety percent purity was the best we could obtain by crystallization of *ante*-C15.

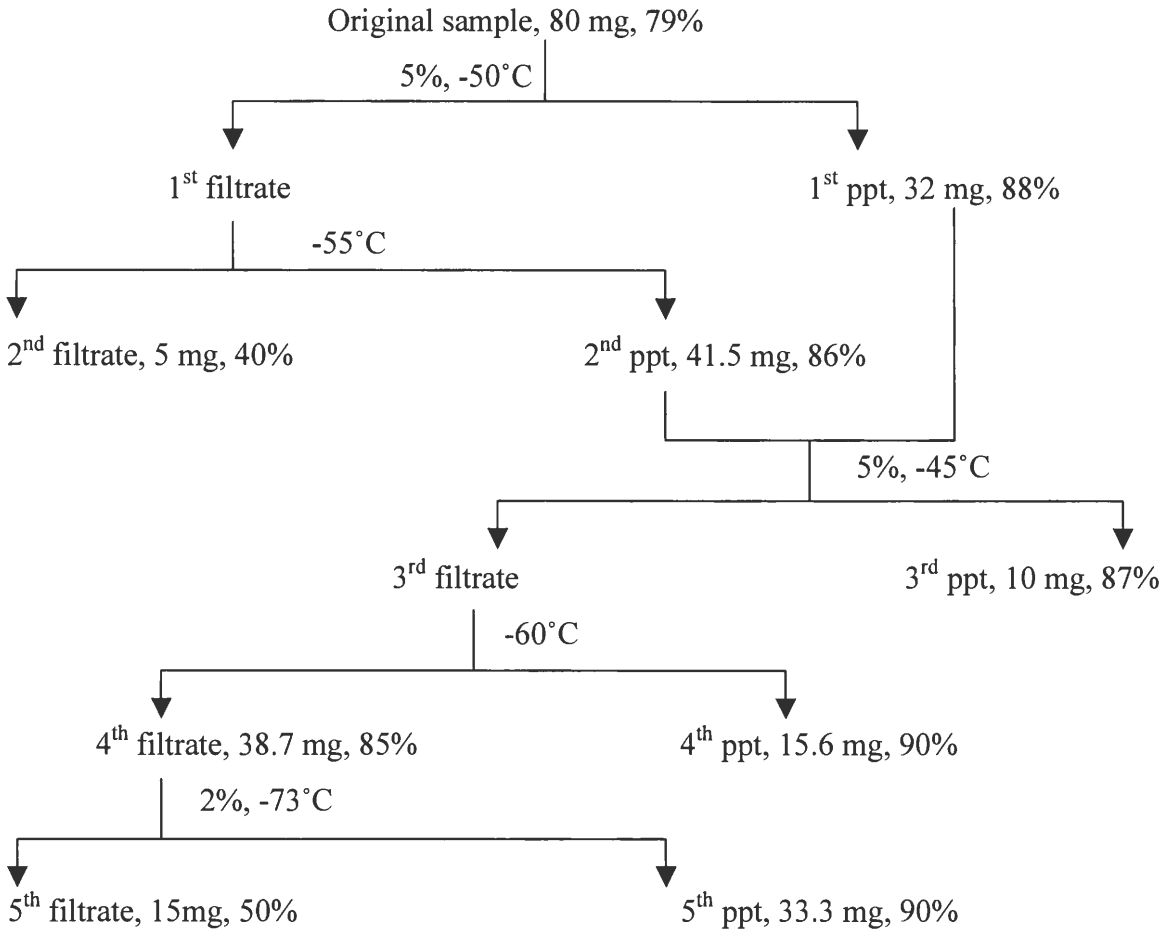

Fig.5. Dry ice-acetone bath crystallization on C15-*anteiso* (preliminary test)

Based on the experience gained from crystallization of *anteiso*-C15, we modified the crystallization procedure by using lower concentration, 2% instead of 5%. The 2% solution of *anteiso*-C17 fraction became cloudy at ~0°C. Visible crystals were observed at -40°C, at

which temperature the first filtration was done. The first precipitate at -40°C was rich in *anteiso*-C17 with 94.8% purity as shown in Fig. 6. The second precipitate at -50˚C was also rich in *anteiso*-C17 with 94.76% purity. The third and fourth precipitate had lower purity as 89.09% and 58.40%. The filtrate was relatively rich in C18:1.

We had expected that high melting point components, i.e. the *iso*-group to precipitate while leaving the lower melting point components, including the *anteiso*- and monounsaturates in the filtrates. i*so*-C14 has a higher melting point than *anteiso*-C15; however, the reverse occurred. Crystallization of *ante*-C17 gave similar result. The *ante*-C17 precipitated and the *iso*-C16 was present in the first two filtrates. Seemingly, when the weight percent of the components in a sample is extremely unbalanced, such as 80% to 10%, the precipitation order will not follow the melting point, but when the components have comparable weight in the mixture, the crystallization will follow the melting point order.

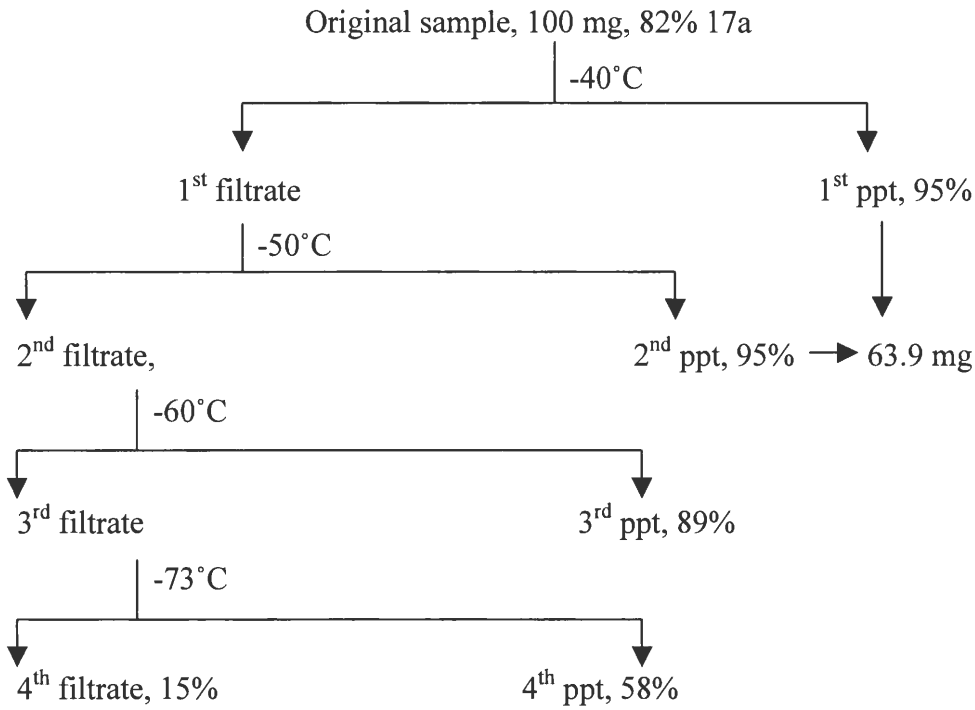

Fig. 6. Dry ice-acetone bath crystallization on *ante*-C17 (preliminary test)

Crystallization on ante-C17 and ante-C13 with modified procedure

Based on our supposition, we modified the procedure to that described previously in the method section. The result of the following crystallization on *ante*-C17 and *ante*-C13 showed the wisdom of this strategy (Fig. 7 and 8). About 97.6% pure *ante*-C17 and 93.7% pure *ante*-C13 were obtained in precipitates. The major impurities in *ante*-C17 sample were *iso*-C16 and C18:1. They were collected in the four filtrates, as shown in Fig.7. *ante*-C11 and *iso*-C12 were major impurities in *ante*-C13 sample, and they tended to stay in filtrates as well (Fig. 8).

Using dry ice-acetone bath, we were able to control the crystallization temperature, and the personnel could operate at room temperature. Another advantage was that we could reach temperature as low as -73˚C that are necessary for the crystallization of short-chain compounds.

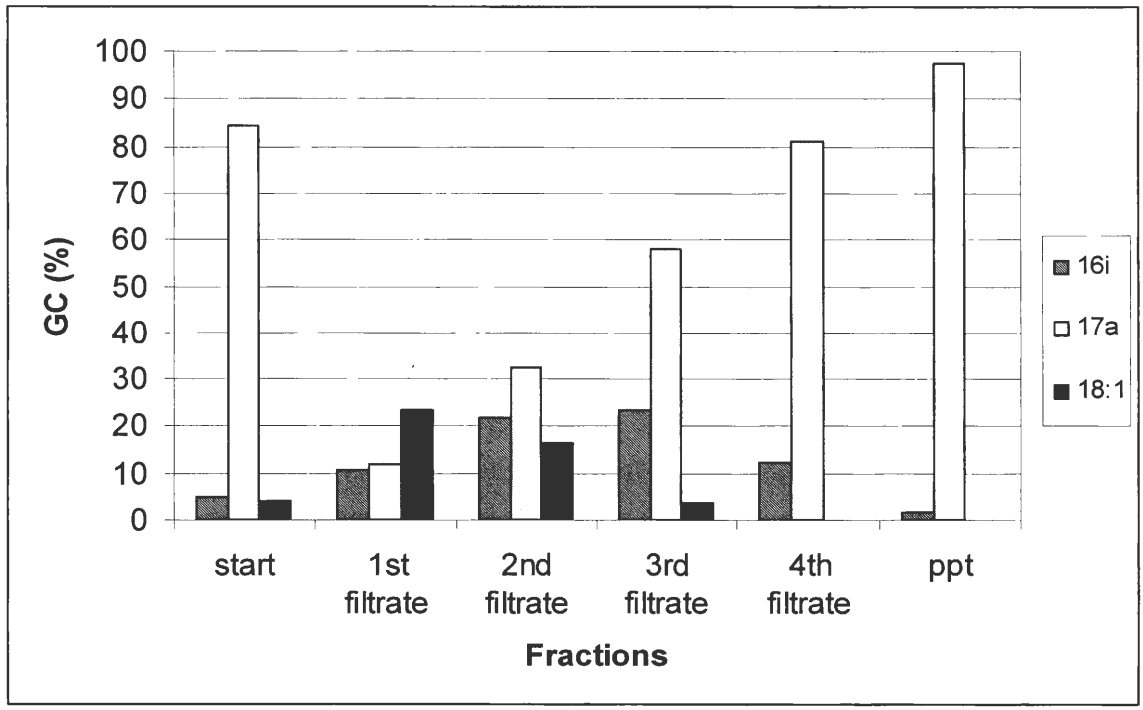

Fig.7. The composition (GC %) of each fraction in the *ante*-C17 crystallization

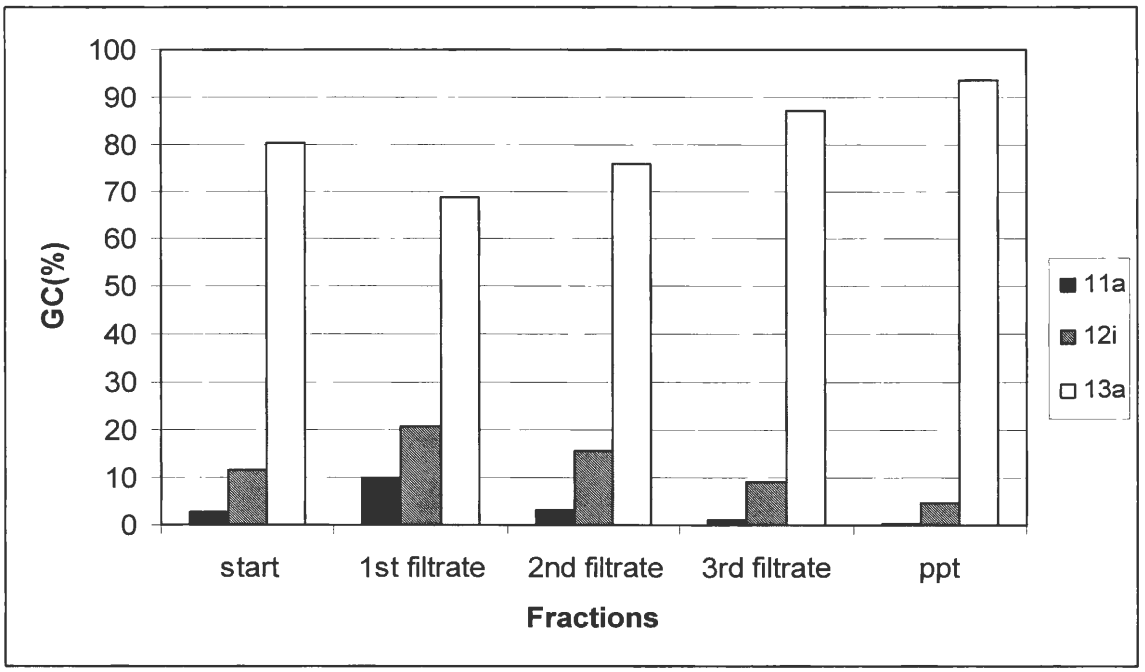

Fig.8. The composition (GC %) of each fraction in the *ante*-C13 crystallization

Transesterification

Preliminary tests on normal chain C12:0 and C18:0 methyl esters gave us clues about the ratio, time, and assistant requirement of the reaction. Two hours reaction time was not enough for completion. Overnight reaction produced FFA and had low yield. Since the results from three hours and four hours reactions were same, we set the reaction time at three hours. From the GC analysis of the isopropyl ester of C12:0, we concluded that the isopropyl ester usually peaked in the GC 1 min later than the corresponding methyl ester. Thus, we identified the isopropyl esters of branched-chain esters as the peaks having this feature.

As shown in Table 15, the branched-chain methyl esters used for transesterification were above 94% pure. The isopropyl esters usually had 1% lower purity, mostly because of

the unreacted methyl esters. The yield of isopropyl ester was not stable in that the trace amount of water in the alcohol hydrolyzed the products.

Table 15. The purity of methyl esters (ME) and isopropyl esters (IE) (GC %)

	Purity of ME	Purity of IE
iso-C18	94.8	95.7
iso-C16	98.3	96.2
iso-C14	94.6	94.2
ante-C17	97.6	96.6
ante-C15	94.8	94.3
ante-C13	93.7	-

Melting points and heats of fusion of methyl esters and isopropyl esters

Fig. 9 shows how onset (T_{on}), completion (T_{com}), and peak value (T_p) of melting were inferred from the DSC melting curve, in which the onset temperature was generated by the computer and is an extrapolation to the baseline of the steepest slope of the peak, and the temperature of completion is set through the same way but on the high temperature side of the peak. This is in accordance with AOCS Official Method Cj 1-94.

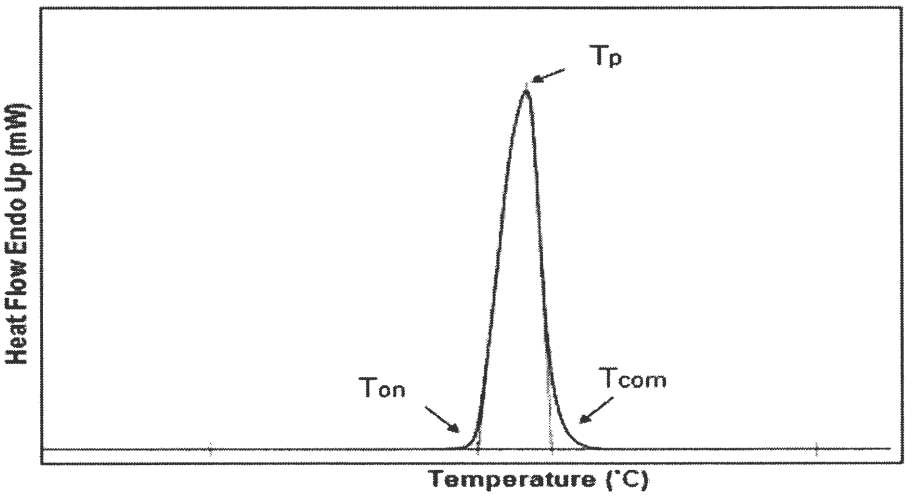

Fig.9. The definition of DSC parameters

According to the AOCS recommended method for the DSC measurement of oils and fats, methyl stearate is to be used as a secondary standard. Its T_{on} and T_{com} were 35.5°C and 39.6°C, respectively. Whereas, the official method reported that the onset temperature should be 39±2°C. The cause for the difference was unknown.

Since the onset temperature may be affected by an impurity, and the melting point of the traditional capillary tube measurement is defined as the temperature at which the solid fat becomes a clear liquid, we should use the completion of melt for comparison with earlier melting point data. Also, the completion of melt is meaningful when evaluating the low temperature performance of potential lubricating oils. The T_{on} , T_{com} , T_p , and ΔH of the methyl and isopropyl esters of various *iso-* and *anteiso-* fatty acids were given in Table 16.

Table 16. The T_{on}, T_{com}, T_p and ΔH of branched-chain methyl esters and isopropyl esters with carbon chain length of 13 to 18

	T_{on}(°C)	T_{com}(°C)	T_p(°C)	ΔH (J/g)
iso-C18-ME	22.8	27.1	25.7	178.2
iso-C16-ME	12.6	18.2	16.5	175.6
iso-C14-ME	-1.5	4.8	2.7	160.4
ante-C17-ME*	0.3	5.2	3.8	154.3
ante-C15-ME*	-14.5	-9.0	-10.9	136.0
ante-C13-ME*	-34.5	-30.5	-31.8	121.8
iso-C18-IE	3.2	7.5	6.3	132.8
iso-C16-IE	-8.3	-3.2	-4.8	127.6
iso-C14-IE*	-21.0	-15.3	-16.9	113.8
ante-C17-IE	-9.3	-5.2	-6.3	113.2
ante-C15-IE	-24.3	-18.1	-20.5	107.2

*showing two peaks on DSC curves

For odd chain methyl esters with 13, 15 and 17 carbon chains, the melting point of the branched-chain methyl ester was depressed sharply compared to the corresponding straight chain methyl esters. The branches lowered the melting points by 36°C, 28°C, 25°C,

respectively (Table 17). For even chain methyl ester with 14, 16, and 18 carbon chains, the lowering of the melting point by 14˚C, 13˚C and 11˚C, respectively, was not as large as those of odd chains. The shorter the chain length of branched esters, the larger was the melting point depression, and an *anteiso-* end groups affected the melting points much more than an *iso-* end group. The observations are reasonable because the influence of the branch end would be more obvious the shorter the chain, and an *anteiso-* group should disrupt carbon chain in the chain packing more than an *iso-* group.

Table 17. The comparison of T_{com} of branched-chain methyl and isopropyl esters with melting points of normal chain FAME

	13	14	15	16	17	18
normal ME[a]	5.8	19.1	19.1	30.7	29.7	37.8
branched ME	-30.5	4.8	-9.0	18.2	5.2	27.1
difference	36.3	14.3	28.1	12.5	24.5	10.7
normal ME[a]	5.8	19.1	19.1	30.7	29.7	37.8
branched IE	-40.0[c]	-15.3	-18.1	-3.2	-5.2	7.5
difference	45.8[c]	34.4	37.2	33.9	34.9	30.3
Normal ME[a]	5.8	19.1	19.1	30.7	29.7	37.8
normal FA[a]	41.8	54.4	52.5	62.9	61.3	70.1
difference	36.0	35.3	33.4	32.2	31.6	32.3
branched ME	-30.5	4.8	-9.0	18.2	5.2	27.1
branched FA[b]	6.2	53.3	23.0	62.4	36.8	69.5
difference	36.7	48.5	32.0	44.2	31.6	42.4

a: from ref. 11
b: from ref. 1
c: estimated values

The addition of an isopropyl ester group lowered the melting points of all the esters below the melting point of their corresponding methyl esters. Compared to straight chain methyl esters, the melting point decrease of odd and even chain isopropyl esters fell in the range of 30˚C~37˚C (Table 17). In the absence of melting point of *ante*-C13-IE, which we

lacked the material to measure, *ante*-C15-IE had the largest decrease - 37˚C. As with the methyl esters, a branch on a shorter chain ester impacted the melting point more than on a longer ester. The similar decrease in the melting points of both odd and even chain isopropyl esters may suggests that when branches are present on both ends of a straight chain methyl ester, the *iso*- and *anteiso*- branches will have similar amount of influence. Although it is not clear that what kind of chain packing crystals of isopropyl-branched esters have, one may imagine that the branches on both ends are quite disruptive to chain alignment.

Typically, the straight chain methyl ester have 32~36˚C lower melting points than the corresponding fatty acids (Table 17). This magnitude of difference also is observed when comparing the odd chain branched methyl esters to branched fatty acids, but for even chains, methyl esters decrease the melting points 10˚C more.

Based on the present data in this study, we estimated that the melting point of *ante*-C13-IE would be around -40˚C.

Plots of the melting points of all the esters show that the melting points of *ante*-ME and iso-IE nearly fell in one line on the graph (Fig.10).

Some of the branched-chain esters showed two peaks on the DSC curve. These esters included *ante*-C13-ME, *ante*-C15-ME, *ante*-C17-ME, and iso-C14-IE, shown in Fig. 11-14 as solid line curves.

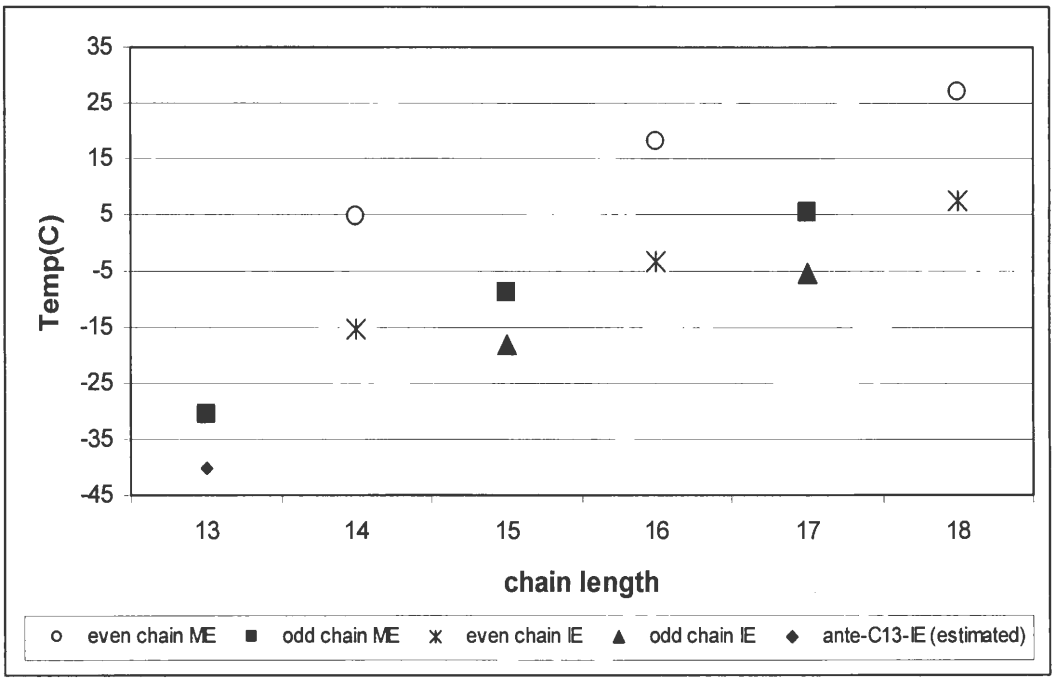

Fig.10. The melting point of methyl ester (ME) and isopropyl ester (IE) of *iso*-C14, C16, C18 and *ante*-C13, C15, C17

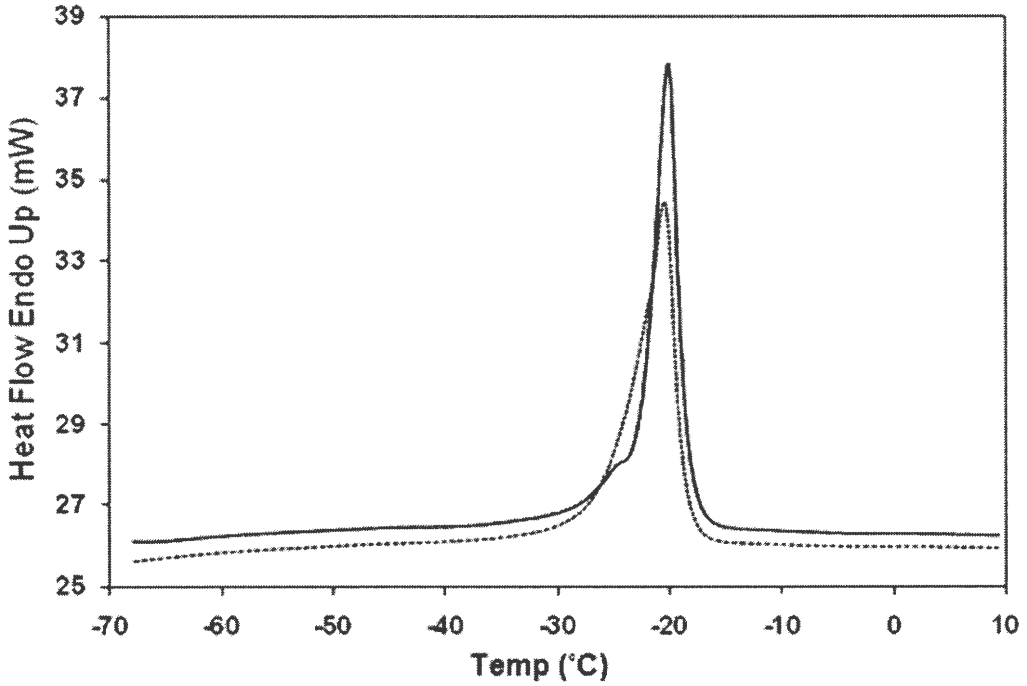

Fig.11. Thermogram of *ante*-C13-ME. Solid line: standard temp. program. Dashed line: modified temperature program.

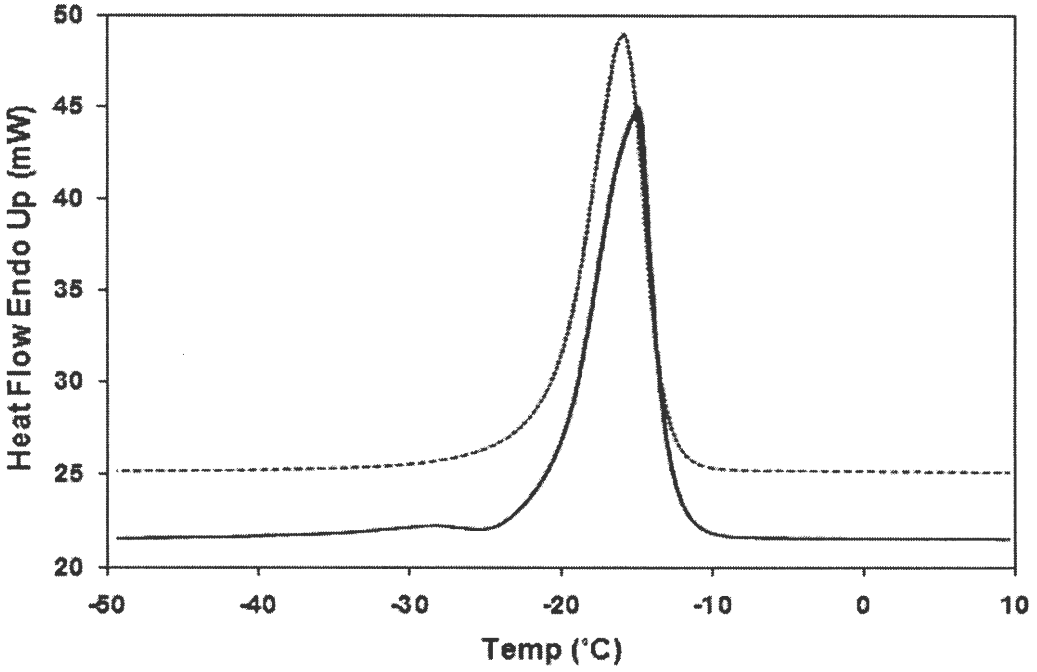

Fig.12. Thermogram of *ante*-C15-ME. Solid line: standard temperature program. Dashed line: modified temperature program.

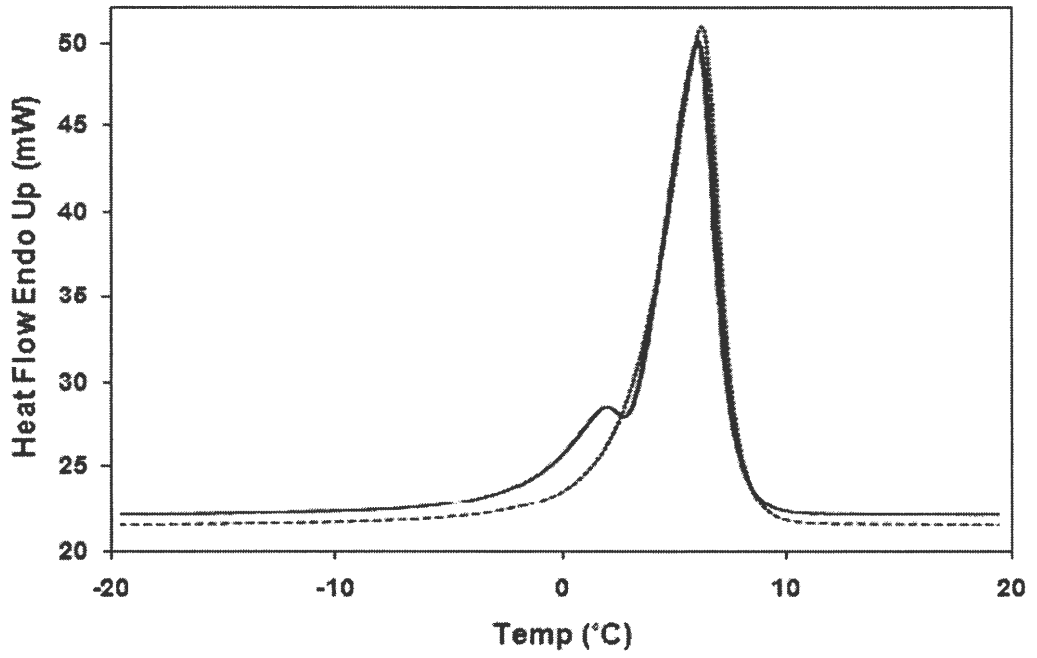

Fig. 13. Thermogram of *ante*-C17-ME. Solid line: standard temperature program. Dashed line: modified temperature program.

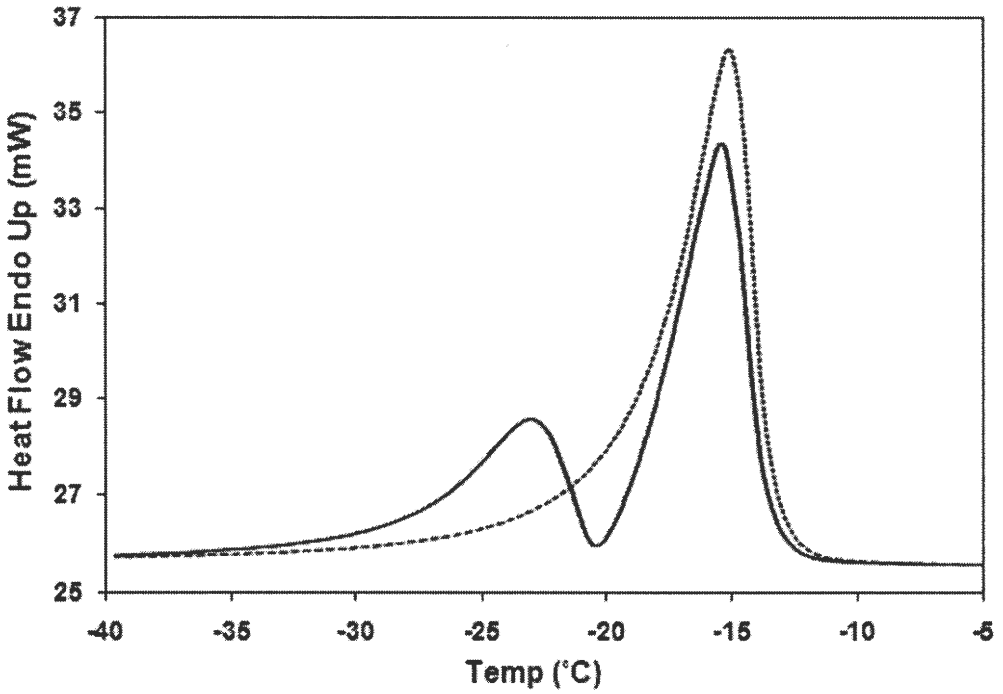

Fig. 14. Thermogram of *iso*-C14-IE. Solid line: standard temperature program. Dashed line: modified temperature program.

This phenomenon seems to be caused by polymorphic behavior. Branched-chain acids have two polymorphic forms, τ and ν (13). The τ form adapts to the branches by forming a highly tilting chain (Fig. 15a). The ν form changes the direction of the branch and then forms a V-shape molecule (Fig. 15b). The τ form is more stable than the ν form and has a higher melting point. Since the purity of most of the samples measured with DSC was 95~98% except *ante*-C13 (93%), and the minor components usually had different melting points from the major component, it was possible that the impurities might be causing the double peaks.

To investigate the cause of the double peaks, we added a special step to the original thermogram. The first heating and cooling steps remained unchanged. But when the sample was reheated, the heat was stopped at the temperature of the intersection of the two peaks.

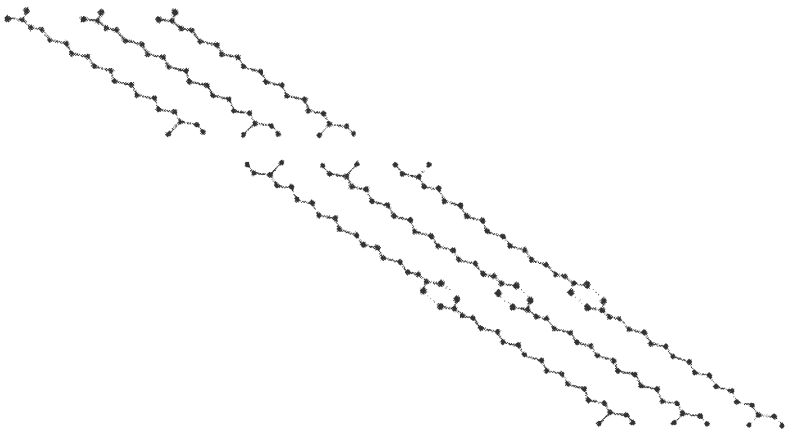

a) 16-*dl*-methyloctadecanoic acid

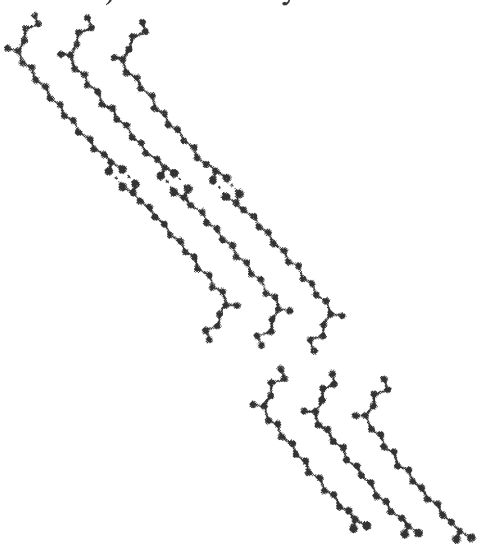

b) 14-*dl*-methyloctadecanoic acid

Fig.15. Crystal Structure of branched-chain fatty acid (Ref. 13).

After equilibration at this temperature for about 2 min, the sample was recooled to -80˚C and held at -80˚C for another 15 min. While reheating to 80˚C at 5˚C/min, the modified temperature program gave one peak on the DSC curve as shown as the dashed line curve in Fig. 11-14. Supposedly, when the temperature reached the melting point of low temperature peak, most of the unstable polymorphic form melted and left the relatively stable form unmelted. Two more minutes' equilibration assured the completeness of melting of unstable

crystals. Then, the stable form crystals functioned as seed crystals in the next circle of crystallization, allowing the crystals to grow on the existing seed crystals and form uniform crystals. The results confirmed this hypothesis that the double peak was caused by polymorphism. The effect of different cooling rates on the crystal formation was also analyzed. Rapid cooling (40˚C/min) produced more crystals having a higher melting point. As shown in Fig. 16, the high melting peak on the solid line curve was larger than the low melting peak. Whereas, slow cooling (2˚C/min) encouraged the growth of the lower melting crystal form, which was indicated in the dashed line curve that the low melting peak was larger.

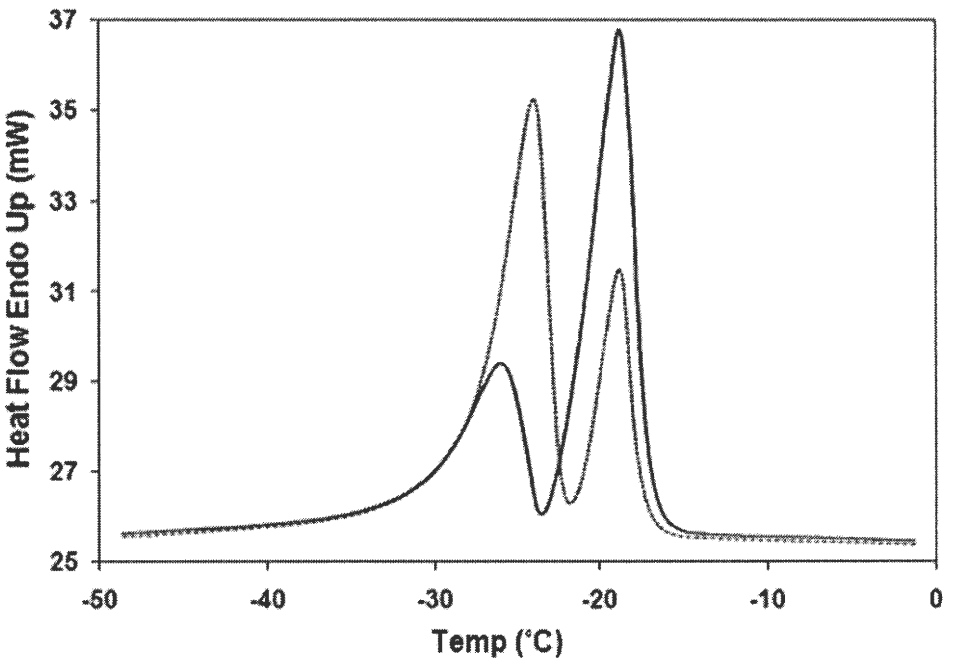

Fig. 16. Thermogram of *iso*-C14-IE. Solid line: 40˚C/min cooling rate in standard temperature program; Dashed line: 2˚C/min cooling rate in standard temperature program

Samples with different purity were measured to see how the minor components affected the melting curve. *ante*-C17-ME of 72% purity and 85% purity were measured with

DSC. The melting peaks on the DSC curves of lower purity samples were observed to shift to lower temperature. The T_p of the 72% sample and the 85% sample were 5.9˚C and 2.4˚C lower, respectively, than that of 95% sample. A single peak was observed in the two less pure samples instead of double peaks.

Among all the branched-chain methyl and isopropyl esters, the lowest T_{com} (-30.5˚C) was observed from *ante*-C13-ME. Other esters melting below 0˚C included *iso*-C16-IE (-3.2˚C), *iso*-C14-IE (-15.3˚C), *ante*-C15-IE (-18.1˚C), *ante*-C15-ME (-9.0˚C), and presumably *ante*-C13-IE (-40˚C) (Table 15). The melting points of these compounds were comparable to and were superior to that of isopropyl soyate produced by Lee *et al.* with isopropyl branches on the ester bond end (9). Especially, the pure product of *ante*-C13-ME would provide satisfactory performance in the coldest weather in Minnesota, of which the tenth percentile minimum ambient temperature was -34˚C in January (9). When blending the isopropyl esters with diesel, the crystallization temperature decreased by ~10˚C (9). Also, we observed the decrease of melting point when the purity of ester was reduced. Therefore, we may expect that other branched compounds mentioned above (melting below 0˚C) would also perform well under extreme weather when they were blended with certain amount of diesel or other esters. The melting points of branched-chain esters and the expectation of blended fuel suggest that it may be an alternative way to solve the problem of low temperature performance of lubricants and biodiesel.

The heats of fusion of each branched-chain ester are listed in Table 15. The value of ΔH increased with the chain length in both odd chain and even chain groups, and in both methyl ester and isopropyl ester groups. The increasing order was C13<C15<C17<C14<C16<C18 (Fig. 17). For straight chain fatty acids, the contribution of –

CH_2 to the heat of fusion is constant when the chain length is greated than 10 (14). But the difference of ΔH between the neighbored two methyl esters and two isopropyl esters of branched-chain acids varied. *Iso*-C18 and *iso*-C16 had very similar ΔH values. The odd chain group had lower ΔH values than the even chain group. The isopropyl ester group had lower ΔH values than the methyl ester group. The difference between methyl and isopropyl esters was about 45 J/g except for *ante*-C15 with 29 J/g.

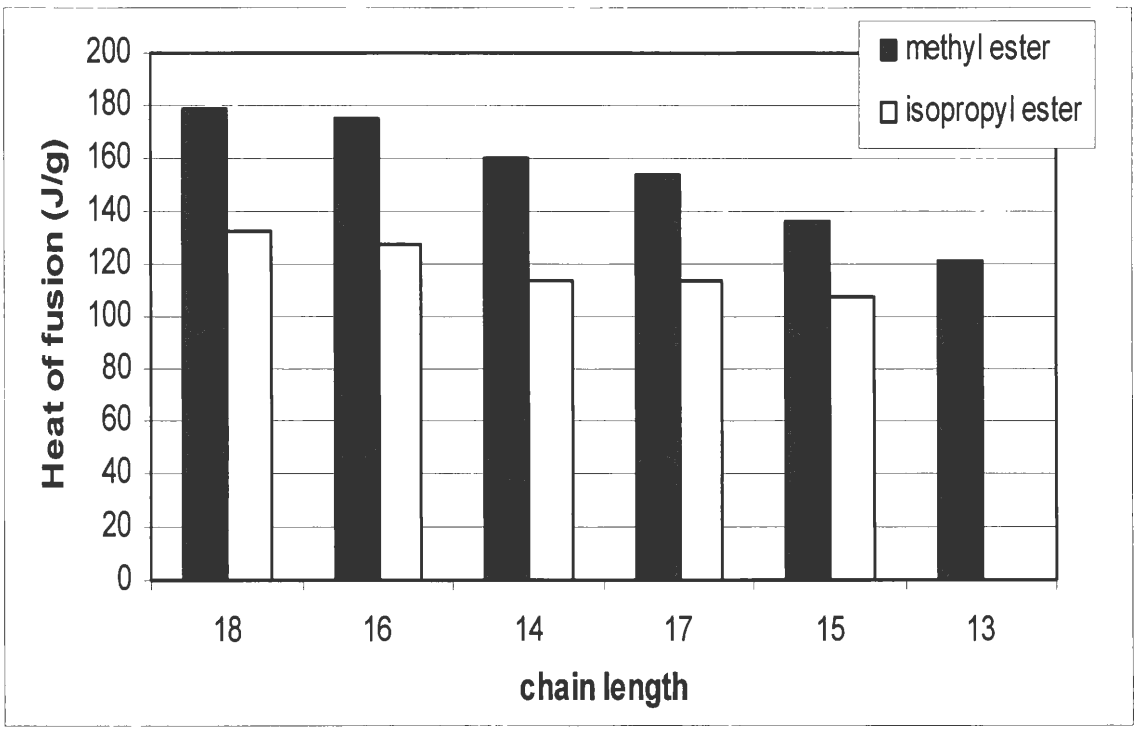

Fig. 17. The heats of fusion of methyl esters (ME) and isopropyl esters (IE) of *iso*-C14, C16, C18 and *ante*-C13, C15, C17

Verification of the structure of branched-chain methyl and isopropyl esters by ^{13}C NMR and ^{1}H NMR

^{13}C NMR

The designation of the carbon atoms in the main chains are shown in Fig. 18. The chemical shifts of the carbon atoms are given in Table 18. Most of the chemical shifts agree

with Gunstone's result with very small variations (44). The difference of C1 signals is caused by the difference between acids and esters. In the carbon atoms assignment model derived from ACD/ChemSketch software, there are two signals with very similar chemical shifts associating with ω2 and ω5 carbon on *anteiso*- chain. But in our spectra, we only observed one signal at 27.11 ppm. The intensity of this signal suggests that one atom is associated with this signal. Gunstone assigned this signal to ω5 and did not assign any signal to ω2. Looking at the environments (i.e. the interactions with surrounding atoms) in which the ω2 and ω5 carbon atoms center, one would expect that these two carbons would give different signals in the NMR spectra. In addition, the assignments of ω3 and ω4 carbons on *anteiso*-chain by software were reverse of Gunstone's. This discrepancy is discussed in HMQC experiment. Although there is some uncertainty, our spectra verified that the compounds we isolated from lanolin were the branched-chain esters we expected.

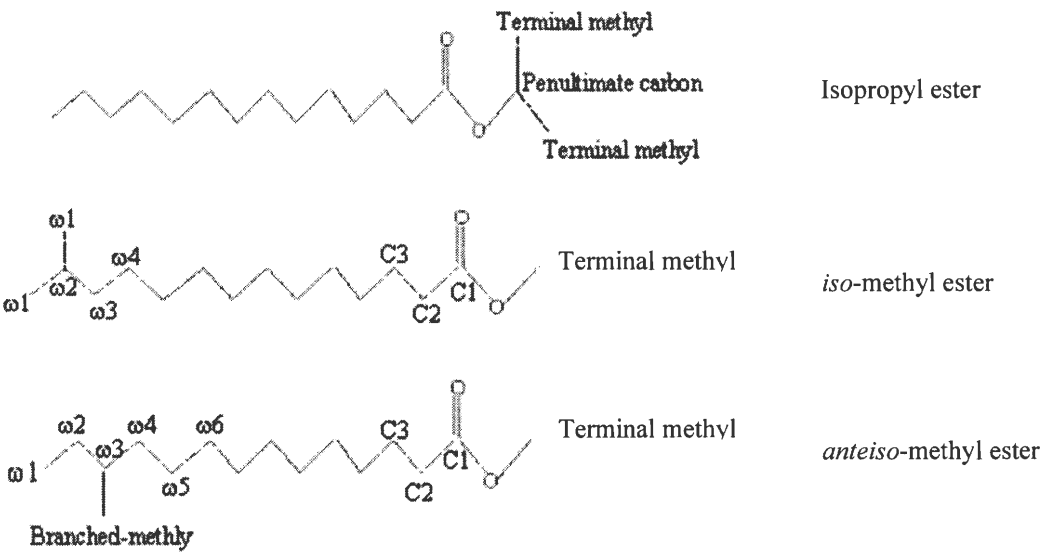

Fig. 18. Designation of the carbon atoms

Table 18. Chemical shifts (ppm) of branched-chain methyl esters and isopropyl esters

	C18i-ME	C17a-ME	C16i-ME	C15a-ME	C14i-ME	C17a-IE	C16i-IE	C15a-IE	C14i-IE	Avg.	ref.
C1, all acids	174.35	174.31	174.46	174.33	174.48	173.53	173.57	173.43	173.43	173.99	180.09
C2, all acids	34.12	34.11	34.12	34.12	34.26	34.39	34.89	34.39	34.73	34.35	34.10
C3, all acids	24.96	24.96	24.96	24.97	25.10	25.06	25.20	25.05	25.05	25.04	24.70
ω1, *iso*	22.68		22.67		22.81		22.82		22.66	22.73	22.68
ω2, *iso*	27.43		27.97		27.56		27.58		27.42	27.59	27.98
ω3, *iso*	39.05		39.05		39.18		39.20		39.04	39.10	39.08
ω4, *iso*	27.97		27.43		28.11		28.12		27.96	27.92	27.45
ω1, *ante*		11.43		11.44		11.44		11.43		11.44	11.42
ω2/ω5, *ante*		27.11		27.11		27.12		27.10		27.11	27.14
ω3, *ante*		34.39		34.39		34.74		34.74		34.57	34.41
ω4, *ante*		36.64		36.63		36.64		36.63		36.64	36.66
ω6, *ante*		30.03		29.93		29.74				29.90	30.06
Branched methyl, *ante*		19.22		19.23		19.23		19.23		19.23	19.23
Terminal methyl, ME	51.46	51.43	51.45	51.45	51.59					51.48	
Terminal methyl, IE						21.86	22.01	21.86	21.86	21.90	
Penultimate methyl						67.28	67.43	67.29	67.28	67.32	
Methylene envelope	29.16-29.95	29.16-29.95	29.16-29.94	29.16-30.01	29.30-30.06	29.13-30.04	29.28-30.10	29.28-30.01	29.12-29.92		28.8-30.0

^{1}H NMR

On ^{1}H NMR spectra, we observed some obvious signal differences between *iso*- and *anteiso*- compounds. Typically, the hydrogen atoms at the methyl ends of *iso*-compounds (i.e. the hydrogen atoms on the two ω1 carbons) gave a doublet signal at 0.85~0.88 ppm, whereas, those at the methyl ends of *anteiso*-compounds (i.e. the hydrogen atoms on the ω1 and branched methyl carbons) gave a asymmetrical triplet signal at the same chemical shift, and normal chain esters showed a symmetrical triplet at the same chemical shift (Fig.19). The other signal difference between *iso*- and *anteiso*- compounds were shown at the region close to the most intensified signal which is associated with hydrogen atoms on the methylene envelope. For *iso*-compounds, we observed a septet peak at ~1.5 ppm which was absent from *anteiso*-compounds' spectra. Based on the experience on NMR that a septet peak is usually caused by the coupling of two methyl groups on an isopropyl compound, we assigned this septet peak to the hydrogen on the carbon at ω2 position of *iso*-branched esters. The intensity of this septet peak indicated that the peak was associated with one proton. The septet peak at difference chemical shift was also observed on the spectra of isopropyl esters which have an isopropyl group at the carboxyl end. The spectra of ante-17-ME sample with 72% purity containing 9.4% C18i and 8.3% C16i also showed a septet peak.

The assignment of signals on ^{1}H NMR provides us a rapid method to differentiate *iso*- and *anteiso*-compounds based on the signal shape of methyl end and the existence of continuous seven-peak at 1.5 ppm. ^{1}H NMR also can be used to detect *iso*- impurity in the *anteiso*-sample.

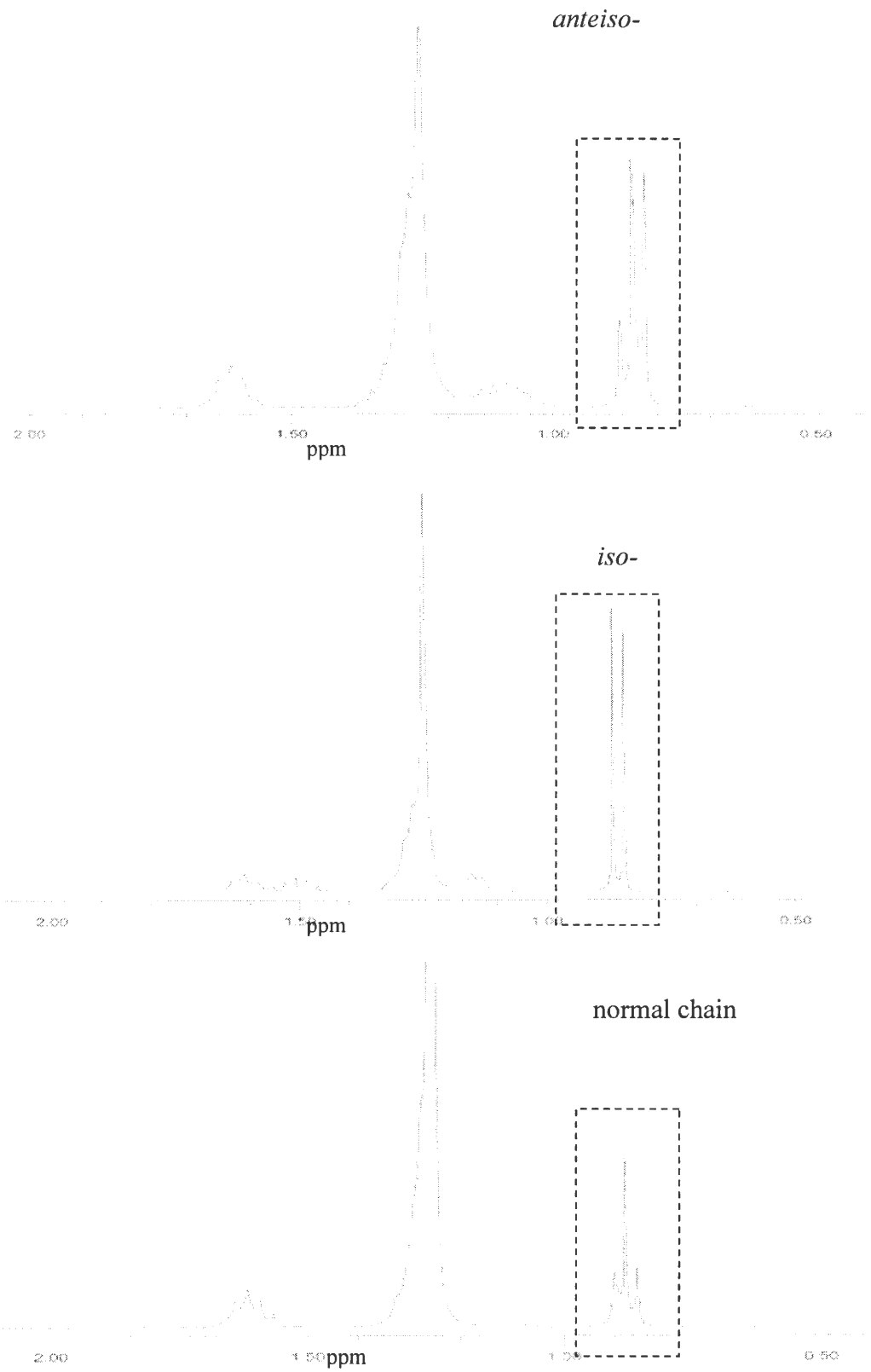

Fig. 19. ^{1}H NMR spectra of *anteiso*-, *iso*-, and normal chain methyl esters

HMQC

In order to correlate the signals on ^{1}H NMR spectra and ^{13}C NMR, we did a HMQC experiment. As shown in Fig.20, the spots on the graph indicated the chemical shifts of C and H bonded. The y-axis is the chemical shift of C, and x-axis is of H. With HMQC, we were able to assign the signals on ^{1}H NMR to their bonded carbons as shown in Fig.21.

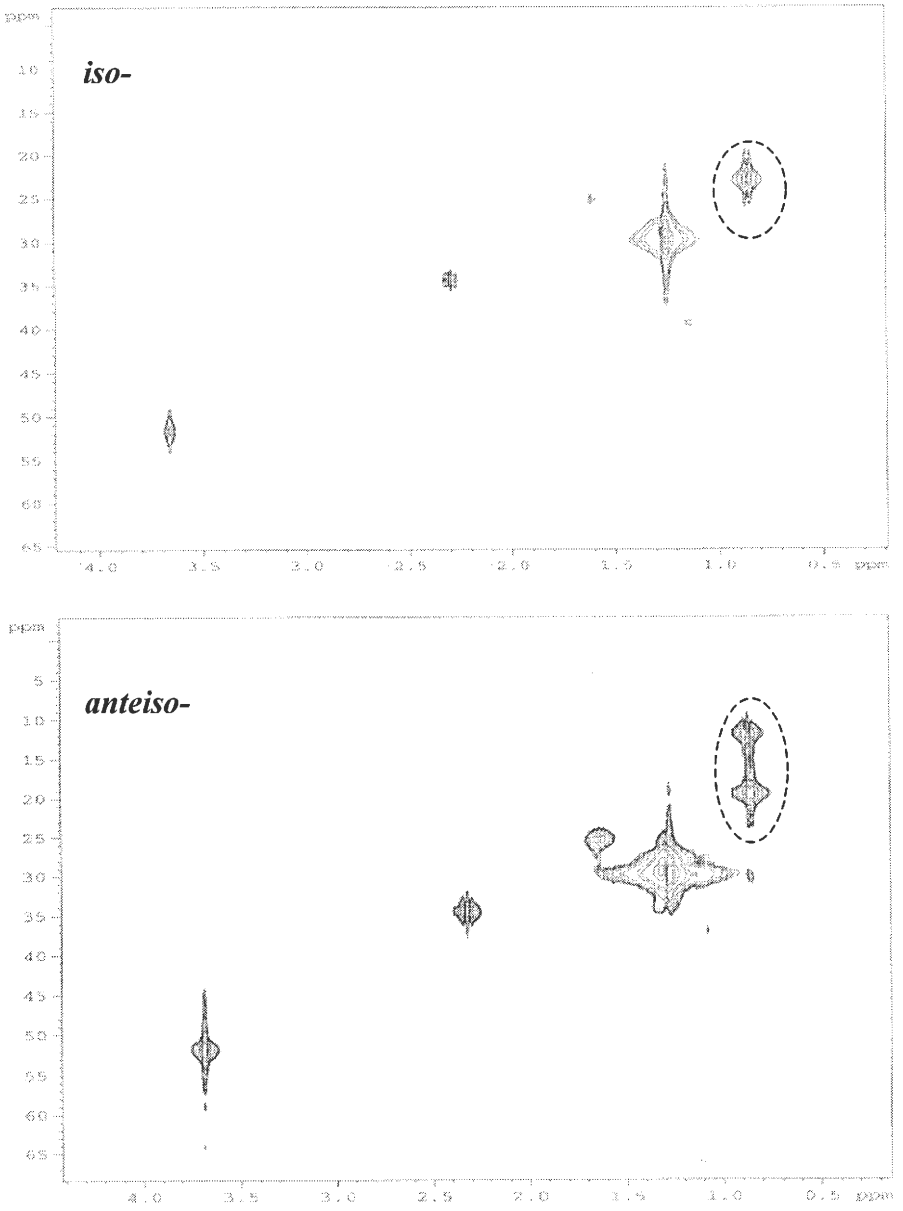

Fig. 20. The HMQC spectra of *anteiso- and iso*-branched methyl esters.

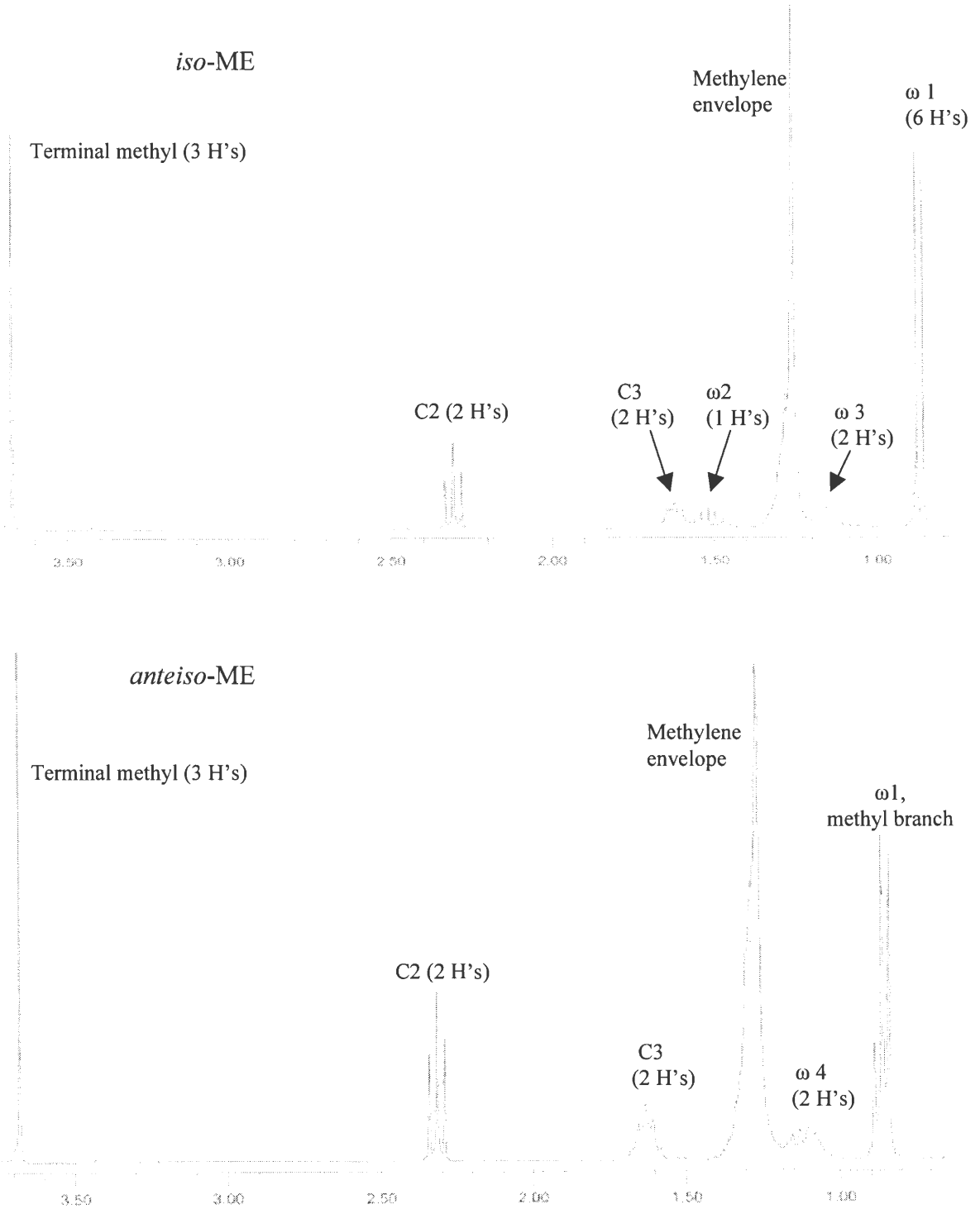

Fig. 21. The assignment of ^{1}H NMR of *iso*- and *anteiso*-ME

Through HMQC experiment, we were able to decide which chemical shift relates to ω3 or ω4 carbon atom. The two-dimensional experiment relates the chemical shift at ~36 on ^{13}C NMR spectra to the chemical shift at ~1.1 on ^{1}H NMR spectra. Since the integration result on ^{1}H NMR spectra indicates that two protons give signal at chemical shift 1.1, we assign ω4 to chemical shift 36.6.

Summary and conclusion

In this study, pure, individual branched-chain fatty acid methyl esters and isopropyl esters with chain length 13 to 18 were isolated from lanolin through spinning band distillation followed by counter-current distribution of the methyl esters with urea and low temperature crystallization with ethyl acetate. This technique separated *iso*- and *anteiso*-branched methyl esters from each other, from normal chain and from unsaturated methyl esters so that we obtained esters of ~ 95% purity. This is an effective procedure to separate branched-chain methyl esters. Transesterification converted methyl esters to isopropyl esters. The melting points and heats of fusion of the methyl esters and isopropyl esters were measure with DSC. The methyl branch, especially the *anteiso*-branch on saturated carbon chain and the isopropyl group on the carboxyl end greatly lower the melting points of esters. The melting points are range from -30.5˚C to 27.1˚C with the lowest melting point (-30.5˚C) of *ante*-C13. ^{13}C NMR spectra verified the structures of most of the branched-chain esters isolated except for *ante*-C13-ME, and *iso*-C18-IE, which were not examined because of lack of materials. The low melting points of branched-chain esters suggest that they may be promising materials for biodiesel because of their low temperature performance.

Goals for future work are to devise scaled-up preparations of the branched esters and provide enough material to determine their lubricant properties and their viscosity profile with temperature. Greater amount of branched esters also allow feeding experiments to determine toxicity and physiological responses. Polyol esters of these acids may provide more typical lubricant viscosities while maintaining a low melting point and stability to oxidation.

Appendix. The coefficient for the reactants ratio of urea and methyl ester

Methyl ester (1 g)	Urea (g)
ante-C19	3.12
iso-C18	3.10
C18:0	3.10
C18:1	3.10
ante-C17	3.08
17:0	3.08
iso-C16	3.06
C16:0	3.06
C16:1	3.06
ante-C15	3.04
C15:0	3.04
iso-C14	3.02
C14:0	3.02
ante-C13	3.00
C13:0	3.00
iso-C12	2.98
C12:0	2.98
ante-C11	2.96
C11:0	2.96
iso-C10	2.94
C10:0	2.94

References

1. Weitkamp, A. W., *J. Am. Chem. Soc.* 67, 447 (1945)
2. Gunstone, F. D., *In* The Lipid Handbook, 2nd ed, Gunstone, F. D., Harwood, J. L. and Padley, F. B. *ed.* 11 (1994)
3. De Navarre, M. G., Chemistry and Manufacture of Cosmetics, 195 (1962)
4. Jewett, B., *Inform*, 14, 528 (2003)
5. Knothe, G., *Inform*, 12, 1103 (2001)
6. http://www.biodiesel.org/resources/fuelfactsheets/default.shtm (Date retrieved 29 April, 2005)
7. Fatemi, S. H. and Hammond, E. G., *Lipids,* 15, 379 (1980)
8. Wong, W. D. and Hammond, E. G., *Lipids,* 12, 475 (1977)
9. Lee, I., Johnson, L. A., and Hammond, E. G., *J. Am. Oil. Chem. Soc.* 72, 1155 (1995)
10. Lee, I., Johnson, L. A., and Hammond, E. G., *J. Am. Oil. Chem. Soc.* 73, 631 (1996)
11. Gunstone, F. D., *In* The Lipid Handbook, 2nd ed, Gunstone, F. D., Harwood, J. L. and Padley, F. B. *ed.* 1 (1994)
12. Hoerr, C. W., *J. Am. Chem. Soc.,* 41, 4 (1964)
13. Hernquvist, L., *In* Crystallization and Polymorphism of fats and fatty acids, Garti, N., and Sato, K. *ed.* 113 (1988)
14. Bailey, A. E. Melting and Solidification of Fats, (1950)
15. Anderson, R. J. and Chargaff, E., *J. Biol. Chem.* 85, 77 (1929-30)
16. Anderson, R. J., *J. Biol. Chem.* 97, 639 (1932)
17. Anderson, R. J., *Yale J. Bios. Med.* 15, 311 (1943)
18. Hansen, R. P., Shorland, F. B. and Cooke, N. J., *Biochem. J.* 50, 581 (1951-52)

19. Hansen, R. P., Shorland, F. B. and Cooke, N. J., *Biochem. J.* 57, 297 (1954)

20. Hansen, R. P., Shorland, F. B. and Cooke, N. J., *Biochem. J.* 64, 214 (1956)

21. Hansen, R. P., Shorland, F. B. and Cooke, N. J., *Biochem. J.* 61, 141 (1955a)

22. Morice, I. M. and Shorland, F. B., *Biochem. J.* 64, 461 (1956)

23. Hansen, R. P., Shorland, F. B. and Cooke, N. J., *Biochem. J.* 61, 547 (1955b)

24. James, A. T. and Wheatley, V. R., *Biochem. J.* 63, 269 (1956)

25. Gunstone, F. D., Fatty Acid and Lipid Chemistry, 12 (1996)

26. Cason, J. and Sumrell, G., *J. Org. Chem.* 16, 1193 (1951c)

27. Abrahamsson, S., Ställberg-Stenhagen, S. and Stenhagen, E., Progress in the chemistry of fats and other lipids, Volume VII, Part I, 31 (1963)

28. Millin, D. J. and Polgar, N., *J. Chem. Soc.* 1902 (1958)

29. Downing, D. T., Kranz, Z. H. and Murray, K. E., *Aust. J. Chem.* 13, 80 (1960)

30. Iverson, J. L., Eisner, J., and Firestone, D., *J. Am. Oil. Chem. Soc.* 42, 1063 (1965)

31. Pelick, N. and Shigley, J. W., *J. Am. Chem. Soc.* 44, 121 (1967)

32. Barnes, C. S., Curtis, R. G., and Hatt, H. H., *Aus. J. Appl. Sci.* 3, 88 (1952)

33. Horn, D. H. S. and Pretorius, Y. Y., *Chem. & Ind.* 1956, R27 (1956)

34. Horn, D. H. S., Hougen, F. W., von Rudloff, R., and Sutton, D. A., *J. Chem. Soc.* 1954, 177 (1954)

35. Horn, D. H. S., Hougen, F. W., von Rudloff, R., *Chem. & Ind.* 106 (1953)

36. Smith Jr., C. R., *In* Topics in Lipid Chemistry, Gunstone, F. D. *ed.* 1, 283 (1970)

37. Gunstone, F. D., Kates, M., and Harwood, J. L., *In* The Lipid Handbook, Gunstone, F. D., Harwood, J. L. and Padley, F. B. *ed.* 225 (1994)

38. Bengen, M.F. Mein Weg zu den neuen Harnstoff-Einschlub-Berbindungen. *Angew. Chem.* 63, 207 (1951)

39. Bengen, M.F. and Schlenk, W., Jr. Uber neuartige Additionsverbindungen des Harnstoffs. *Experientia* 5, 200 (1949)

40. Hayes, D. G., *Inform,* 13, 781 (2002)

41. Hayes, D. G., *Inform,* 13, 832 (2002)

42. Sumerwell, W. N., *J. Am. Chem. Soc.* 79, 3411 (1957)

43. Singleton, W. S., *In* Fatty Acids, Markley, K. S. *ed*. Part I. 522 (1964)

44. Gunstone, F.D., *Chem. Phys. Lipids.* 65, 155 (1993)

Acknowledgement

I would like to appreciate my advisor, Dr. Earl Hammond, for his guidance, support and encouragement in the past two years. For me, he is more like a knowledgeable, kind and humorous grandpa than just a teacher. I learned so much from him. I always feel that I was such a lucky guy to become one of his students.

I would like to appreciate my parents. What they gave me is priceless. They always believe that their daughter will become somebody. As a single child in my family, I owe them too much. What I have done, what I am doing, and what I will do, is trying to make them be proud of me.

I would like to appreciate my friends both in China and in US. They are so supportive and ready to give me a hand all the time. They made my life colorful. With them, I will never feel lonely.